



Polymorphisms in Human Cytomegalovirus Glycoprotein O (gO) Exert Epistatic Influences on Cell-Free and Cell-to-Cell Spread and Antibody Neutralization on gH Epitopes

Le Zhang Day,^{c,d} Cora Stegmann,^{a,d} Eric P. Schultz,^{a,b,d} Jean-Marc Lanchy,^{a,d} Qin Yu,^{a,d}  Brent J. Ryckman^{a,b,c,d}

^aDivision of Biological Sciences, University of Montana, Missoula, Montana, USA

^bCellular, Molecular and Microbial Biology Program, University of Montana, Missoula, Montana, USA

^cBiochemistry and Biophysics Program, University of Montana, Missoula, Montana, USA

^dCenter for Biomolecular Structure and Dynamics, University of Montana, Missoula, Montana, USA

ABSTRACT Human cytomegalovirus (HCMV) glycoproteins H and L (gH/gL) can be bound by either gO or the UL128 to UL131 proteins (referred to here as UL128-131) to form complexes that facilitate entry and spread, and the complexes formed are important targets of neutralizing antibodies. Strains of HCMV vary considerably in the levels of gH/gL/gO and gH/gL/UL128-131, and this can impact infectivity and cell tropism. In this study, we investigated how natural interstrain variation in the amino acid sequence of gO influences the biology of HCMV. Heterologous gO recombinants were constructed in which 6 of the 8 alleles or genotypes (GT) of gO were analyzed in the backgrounds of strains TR and Merlin (ME). The levels of gH/gL complexes were not affected, but there were impacts on entry, spread, and neutralization by anti-gH antibodies. AD169 (AD) gO (GT1a) [referred to here as ADgO(GT1a)] drastically reduced cell-free infectivity of both strains on fibroblasts and epithelial cells. PHgO(GT2a) increased cell-free infectivity of TR in both cell types, but spread in fibroblasts was impaired. In contrast, spread of ME in both cell types was enhanced by Towne (TN) gO (GT4), despite similar cell-free infectivity. TR expressing TNgO(GT4) was resistant to neutralization by anti-gH antibodies AP86 and 14-4b, whereas ADgO(GT1a) conferred resistance to 14-4b but enhanced neutralization by AP86. Conversely, ME expressing ADgO(GT1a) was more resistant to 14-4b. These results suggest that (i) there are mechanistically distinct roles for gH/gL/gO in cell-free and cell-to-cell spread, (ii) gO isoforms can differentially shield the virus from neutralizing antibodies, and (iii) effects of gO polymorphisms are epistatically dependent on other variable loci.

IMPORTANCE Advances in HCMV population genetics have greatly outpaced understanding of the links between genetic diversity and phenotypic variation. Moreover, recombination between genotypes may shuffle variable loci into various combinations with unknown outcomes. UL74(gO) is an important determinant of HCMV infectivity and one of the most diverse loci in the viral genome. By analyzing interstrain heterologous UL74(gO) recombinants, we showed that gO diversity can have dramatic impacts on cell-free and cell-to-cell spread as well as on antibody neutralization and that the manifestation of these impacts can be subject to epistatic influences of the global genetic background. These results highlight the potential limitations of laboratory studies of HCMV biology that use single, isolated genotypes or strains.

KEYWORDS antibody neutralization, cytomegalovirus, entry, epistasis, genetic diversity, glycoproteins, spread, tropism

Citation Day LZ, Stegmann C, Schultz EP, Lanchy J-M, Yu Q, Ryckman BJ. 2020. Polymorphisms in human cytomegalovirus glycoprotein O (gO) exert epistatic influences on cell-free and cell-to-cell spread and antibody neutralization on gH epitopes. *J Virol* 94:e02051-19. <https://doi.org/10.1128/JVI.02051-19>.

Editor Richard M. Longnecker, Northwestern University

Copyright © 2020 American Society for Microbiology. All Rights Reserved.

Address correspondence to Brent J. Ryckman, brent.ryckman@mso.umt.edu.

Received 4 December 2019

Accepted 24 January 2020

Accepted manuscript posted online 29 January 2020

Published 31 March 2020

Recent application of state-of-the-art genomics approaches have begun to uncover a greater and more complex genetic diversity of human cytomegalovirus (HCMV) than had been appreciated (1–8). Of the 165 canonical open reading frames (ORFs) in the 235-kbp HCMV genome, 21 show particularly high nucleotide diversity and are distributed throughout the otherwise highly conserved genome. Links between specific genotypes and observed phenotypes are not well understood, and as a corollary outcome, the factors driving HCMV genetic diversity and evolution remain speculative. This is further complicated by recombination between genotypes that can shuffle the diverse loci into various combinations, and this may result in epistasis where the phenotypic manifestation of a specific genotype of one locus may be influenced by the specific genotypes of other loci. Thus, realizing the full potential of modern genomics approaches toward the design of new interventions, clinical assessments, and predictions will require better mechanistic understanding of the links between genotypes and phenotypes.

The UL74 ORF codes for glycoprotein O (gO) [the UL74-encoded gO is referred to here as UL74(gO)] and is one of the aforementioned highly diverse loci of HCMV (9–12). Most phylogenetic groupings indicate 8 genotypes or alleles of gO that differ in 10 to 30% of amino acids, predominately near the N terminus and in a short central region. These amino acid polymorphisms also affect predicted N-linked glycan sites. The evolutionary origins of gO genotype diversity are not understood. Studies that followed infected humans through latency-reactivation cycles over several years demonstrated remarkable stability in UL74(gO) sequences, arguing against the idea of selective pressure from a dynamically adapting host immune system as a driving force for gO diversity (11, 13). The functional significance of gO diversity has only recently been addressed and centers around its role as a subunit of the envelope glycoprotein complex gH/gL/gO, which is involved in the initiation of infection into different cell types.

The general model for herpesvirus entry involves fusion between the virion envelope and cell membranes mediated by the fusion protein gB and the regulatory protein gH/gL (14–16). The HCMV gH/gL can be unbound, or bound by gO or the set of proteins UL128 to UL131 (referred to here as UL128-131) (17–20). How these gH/gL complexes participate to mediate infection is complicated and seems to depend on both the cell type and whether the infection is by cell-free virus or direct cell-to-cell spread. Efficient infection of all cultured cell types by cell-free HCMV is dependent on gH/gL/gO, whereas infection of certain cell types, including epithelial and endothelial cells, additionally requires gH/gL/UL128-131 (21–26). Experiments involving HCMV mutants lacking either gO or proteins UL128-131 suggested that cell-to-cell spread in fibroblast cultures can be mediated by either gH/gL/gO or gH/gL/UL128-131, whereas in endothelial and epithelial cells gH/gL/UL128-131 is required, and it has remained unclear whether gH/gL/gO plays any role (23, 25, 27, 28). While it is clear that gH/gL/gO can bind to the cell surface protein platelet-derived growth factor receptor alpha (PDGFR α) via gO and that gH/gL/UL128-131 can bind NRP2 and OR1411 via UL128-131, the specific function(s) of these receptor engagements is unclear; it may include virion attachment, regulation of gB fusion activity, or activation of signal transduction pathways (29–31). In the case of gH/gL/gO, binding to PDGFR α activates signaling pathways, but these are not required for entry (28, 30, 32). Stegmann et al. showed that binding of a gO-null HCMV to fibroblasts and endothelial cells was impaired, yet it is unclear whether this was due to lack of PDGFR α engagement (33). Finally, Wu et al. reported coimmunoprecipitation of gB with gH/gL/gO and PDGFR α , consistent with a role for the gH/gL/gO-PDGFR α interaction in promoting gB fusion activity (32). However, unbound gH/gL has been shown to mediate cell-cell fusion and has also been found in a stable complex with gB in extracts of infected cells and extracellular virions (20, 34). Thus, although many of the key factors in HCMV entry and cell-to-cell spread have been identified, their interplay in the various entry pathways is unclear. Moreover, the influence of gO diversity remains a mystery.

The gH/gL complexes have been extensively studied as potential vaccine candi-

dates, and neutralizing antibodies have been described that react with epitopes on gH/gL, on UL128-131, and on gO (35–43). Anti-UL128-131 antibodies neutralize with high potency but only on cell types for which gH/gL/UL128-131 is required for entry, e.g., epithelial cells. In contrast, antibodies that react with epitopes on gH/gL tend to neutralize virus on both fibroblasts and epithelial cells but are far less potent on fibroblasts, where only gH/gL/gO is needed for entry. One explanation for these observations is that gO, with its extensive N-linked glycan decorations, presents more steric hindrance to antibodies accessing the underlying gH/gL epitopes than do the UL128-131 proteins. Similar effects of glycans in shielding neutralizing epitopes have been described for HIV Env and for HCMV gN (44, 45). In support of this hypothesis for gO, Jiang et al. showed that focal spread of a gO null HCMV in fibroblasts was more sensitive to anti-gH antibodies (46). Recently, Cui et al. described antibodies that reacted to a linear epitope on gH and exhibited strain-selective neutralization that could not be explained by polymorphisms within the gH epitope (47). One possible explanation was that gO polymorphisms between the strains imposed differential steric hindrances on these antibodies.

In this study, we utilized a set of HCMV bacterial artificial chromosome (BAC) clones that represent the range of phenotypic diversity in terms of gH/gL complexes. HCMV TB40/e (TB), TR, and Merlin (ME) differ dramatically in the amounts of gH/gL complexes in the virion envelope and their infectivities on fibroblasts and epithelial cells. Extracellular virions of TB and TR contain gH/gL predominately in the form of gH/gL/gO and are far more infectious on both fibroblasts and epithelial cells than ME, which contains overall smaller amounts of gH/gL, predominately as gH/gL/UL128-131 (9, 26). Each of these strains encodes a different representative of the 8 gO genotypes. In a previous study, we demonstrated that variation in the UL74(gO) ORF was not responsible for the observed differences between TR and ME (48). Rather, it was shown that the amounts of gH/gL/gO in ME and TR virions were influenced by different steady-state levels of gO present during progeny assembly. Kalsner et al. showed that replacing the gO of TB with that of Towne (TN) also did not affect the levels of gH/gL complexes but may have enhanced the ability of TB to spread in epithelial cell cultures (49). In this study, we have generated a set of heterologous gO recombinants to include 6 of the 8 genotypes in the genetic backgrounds of the gH/gL/gO-rich strain TR and the gH/gL/UL128-131-rich ME to analyze how the differences in gO sequence influence HCMV biology. The results demonstrate that gO variation can have dramatic effects on cell-free entry, cell-to-cell spread, and neutralization by anti-gH antibodies. In some cases, opposite influences were observed for a given gO genotype in the different backgrounds of TR and ME, indicating epistasis with other genetic differences between these strains.

RESULTS

Influences of gO polymorphisms on cell-free infectivity and tropism can be dependent on the background strain. To examine the effects of gO polymorphism, a set of recombinant viruses was constructed in which the endogenous UL74(gO) ORFs of strain TR and ME were replaced with the UL74(gO) ORFs from 5 other strains. BAC-cloned strains TR and ME were chosen as the backgrounds for these studies since they represent gH/gL/gO-rich and gH/gL/UL128-131-rich strains, respectively (9, 26, 49). Additionally, ME is restricted to a cell-to-cell mode of spread in culture, whereas TR is capable of both cell-free and cell-to-cell modes of spread (23, 50, 51). The intended changes to UL74(gO) in each recombinant BAC were verified by sequencing the UL74 ORF, and the flanking regions used for BAC recombineering. However, it was recently reported that HCMV BAC clones can sustain various genetic deletions, rearrangements, and mutations during rescue in fibroblasts or epithelial cells, resulting in mixed-genotype populations (52). To ensure that phenotypes characterized were associated with the intended changes to UL74(gO) and not with other genetic changes sustained during BAC rescue in fibroblasts, all analyses were performed on at least three independently BAC-rescued viral stocks.

Background genotype:

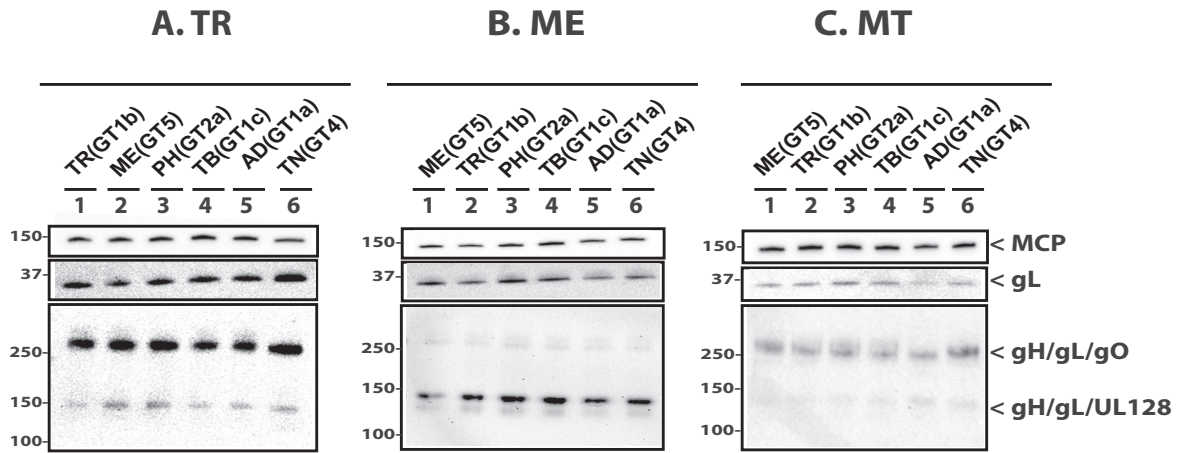


FIG 1 Immunoblot analysis of gH/gL complexes in parental and heterologous gO recombinant HCMV. Equal number of cell-free virions (as determined by qPCR) of HCMV TR (A), ME (B), or MT (C) or the corresponding heterologous gO recombinants were separated by reducing (upper two panes) or nonreducing (bottom pane) SDS-PAGE and analyzed by immunoblotting with antibodies specific for major capsid protein (MCP) or gL. Blots shown are representative of three independent experiments. Molecular mass markers (in kilodaltons) are indicated on each panel.

As a basis for interpretation of the later biological comparisons among recombinants, the levels of gH/gL complexes incorporated into the virion envelope were analyzed by immunoblotting as previously described (9, 26). As in the previous studies, TR contained predominantly gH/gL/gO, whereas ME contained mostly gH/gL/UL128-131 (Fig. 1, compare lanes 1 in panels A and B). Propagation of ME under conditions of UL131 transcriptional repression resulted in virions with more gH/gL/gO and less gH/gL/UL128-131 as previously described (Fig. 1C, lane 1) (26, 51). ME virions generated in this manner were designated MT (“Merlin-T”). Some minor differences in the amounts of total gL, gH/gL/gO, and gH/gL/UL128-131 were observed for some of the heterologous gO recombinants relative to their parental strains. However, band density analyses showed that all apparent differences were less than 3-fold and few reached statistical significance compared across multiple experiments, likely reflecting the limitations of immunoblotting as a precise quantitative method, as well as stock-to-stock variability in glycoprotein composition (Table 1). Thus, consistent with our previous report, differences between strains TR and ME in the abundance of gH/gL complexes are predominately influenced by genetic background differences outside the UL74(gO) ORF (48).

While gH/gL/gO is clearly important for entry into both fibroblasts and epithelial cells, the mechanisms are likely different since (i) fibroblasts clearly express the gH/gL/gO receptor PDGFR α on their surface, whereas ARPE19 epithelial cells express little or none of this protein (28, 30, 32, 53), and (ii) entry into epithelial cells requires gH/gL/UL128-131 in addition to gH/gL/gO (23, 24, 26). Thus, it was possible that gO polymorphisms would differentially affect replication in these two cell types. To address this, fibroblast-to-epithelial cell tropism ratios were determined for each parental strain and gO recombinant by inoculating cultures of fibroblasts and epithelial cells in parallel with equivalent amounts of cell-free virus stocks. The number of infected cells in each culture was then determined by flow cytometry using green fluorescent protein (GFP) expressed from the virus genome. Figure 2 shows the results of these experiments as the fold preference for either cell type as a ratio, where “1” indicates equal infection of both cell types. Stocks of the parental TR were approximately 20-fold more infectious on fibroblasts than on epithelial cells (Fig. 2A). Preference toward fibroblasts was greater for TR recombinants expressing gO (GT5) of strain ME [referred to here as MEgO(GT5)], PHgO(GT2a), and TBgO(GT1c). In contrast, tropism ratios of TR recombinants expressing AD169 (AD) gO (GT1a) [referred to here as ADgO(GT1a)] and Towne (TN) gO (GT4) [referred to here as TNgO(GT4)] were closer to 1, indicating more equal infection of both cell types. Parental ME and all of the ME-based gO recombinants had

TABLE 1 Immunoblot band density analyses of parental and heterologous gO recombinants

Virus ^a	Virion protein(s)							
	MCP		gL		gH/gL/gO		gH/gL/UL128	
	Fold ^b	ANOVA ^c	Fold	ANOVA	Fold	ANOVA	Fold	ANOVA
TR_TR(GT1b)	1.0	—	1.0	—	1.0	—	1.0	—
TR_MEgO(GT5)	1.1	NS	0.6	NS	1.4	NS	2.0	NS
TR_PHgO(GT2a)	1.1	NS	0.9	NS	1.8	NS	2.3	*
TR_TBgO(GT1c)	1.2	NS	0.8	NS	0.9	NS	0.9	NS
TR_ADgO(GT1a)	1.1	NS	0.9	NS	0.9	NS	1.0	NS
TR_TNgO(GT4)	1.1	NS	2.0	NS	2.7	NS	2.1	NS
ME_MEgO(GT5)	1.0	—	1.0	—	1.0	—	1.0	—
ME_TR(GT1b)	0.9	NS	0.8	NS	0.9	NS	1.1	NS
ME_PHgO(GT2a)	1.1	NS	1.1	NS	1.4	NS	1.4	NS
ME_TBgO(GT1c)	1.3	NS	1.2	NS	1.0	NS	1.4	NS
ME_ADgO(GT1a)	1.0	NS	0.7	NS	0.9	NS	1.1	NS
ME_TNgO(GT4)	1.1	NS	0.8	NS	0.9	NS	1.4	NS
MT_MEgO(GT5)	1.0	—	1.0	—	1.0	—	1.0	—
MT_TR(GT1b)	1.1	NS	1.2	NS	0.7	NS	0.9	NS
MT_PHgO(GT2a)	1.1	NS	1.6	NS	1.4	NS	1.1	NS
MT_TBgO(GT1c)	1.1	NS	1.3	NS	1.1	NS	1.6	NS
MT_ADgO(GT1a)	0.8	NS	0.5	NS	0.6	NS	1.7	NS
MT_TNgO(GT4)	0.9	NS	0.7	NS	1.4	NS	1.8	NS

^aThree independent stocks of cell-free virions collected from infected nHDF (for TR and ME) or HFFftet (for MT) culture supernatants and analyzed by immunoblotting as described for Fig. 1.

^bMean fold difference of chemiluminescent band densities obtained for each recombinant compared to the parental TR in three independent experiments.

^cOne-way ANOVA with Dunnett's multiple-comparison test comparing each recombinant to the parental in three independent experiments. *, $P \leq 0.05$. —, value not calculated. NS, not significant.

tropism ratios within the range of 6 in favor of fibroblasts to 3 in favor of epithelial cells. Several of these viruses had variability between replicate stocks where some had slight fibroblast preference and others slight epithelial cell preference (Fig. 2B). Propagation of the ME-based viruses as MT greatly increased the preference toward fibroblast

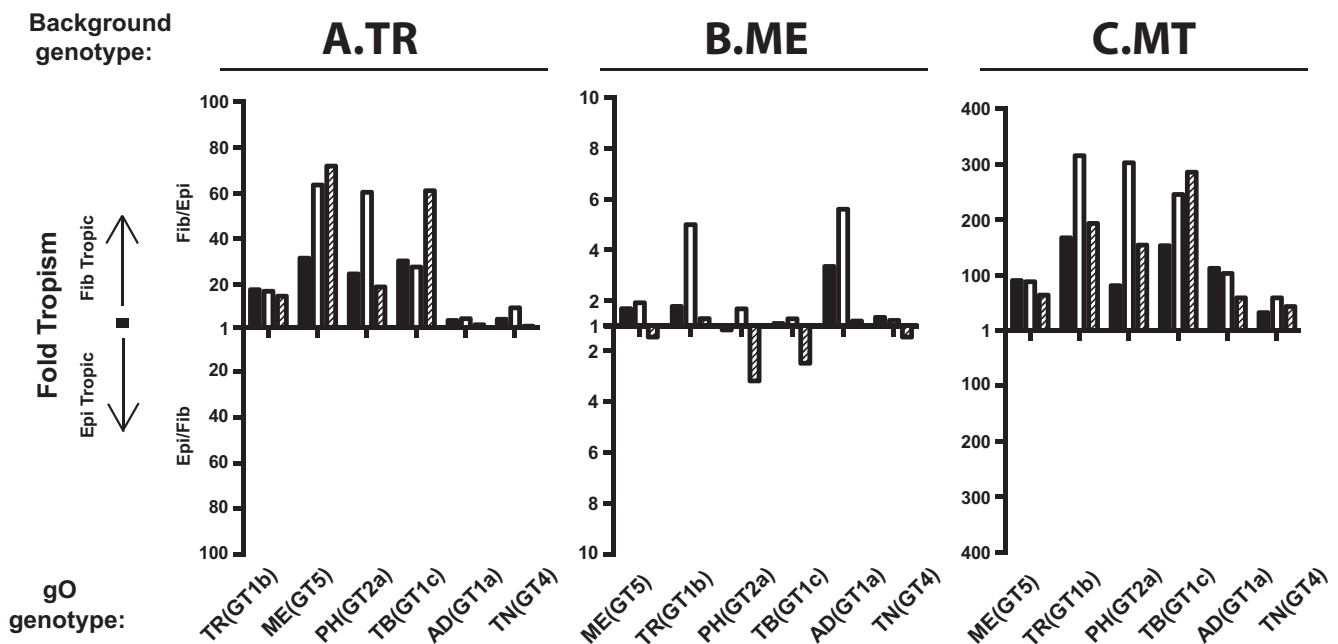


FIG 2 Relative fibroblast and epithelial cell tropism of parental and heterologous gO recombinant HCMV. Cell-free stocks of HCMV TR (A), ME (B), or MT (C) or the corresponding heterologous gO recombinants were serially diluted, and side-by-side cultures of nHDF (Fib) and ARPE19 epithelial cells (Epi) were inoculated with equal volumes of the dilutions. The number of infected cells was determined by flow cytometry for GFP at 2 days postinfection. Ratios greater than or equal to 1 of the number of each cell type infected (Fib/Epi or Epi/Fib) are plotted for each of three independent sets of virus stocks (black, open, and hatched bars).

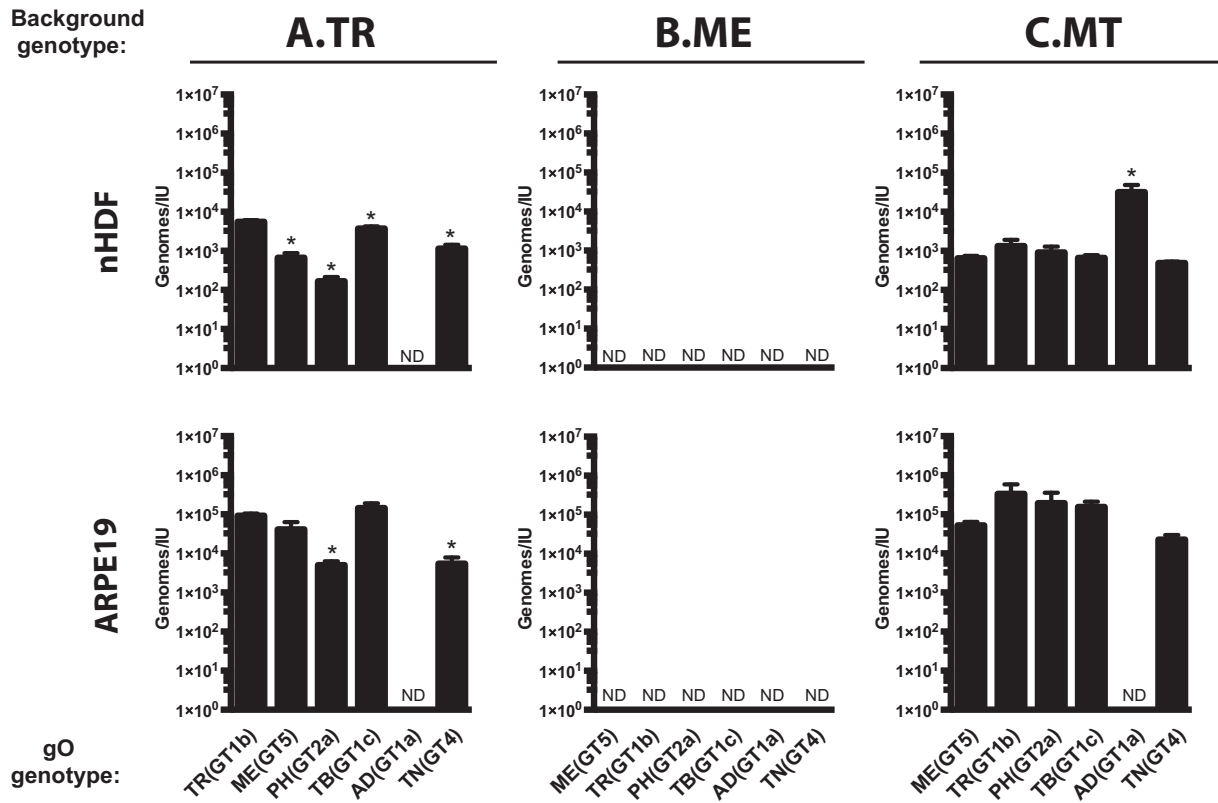


FIG 3 Specific infectivity of parental and heterologous gO recombinant HCMV. Extracellular HCMV stocks of HCMV TR (A), ME (B), or MT (C) or the corresponding heterologous gO recombinants were quantified by qPCR for viral genomes, and infectious units (IU) were determined by flow cytometry quantification of GFP-expressing nHDF or ARPE-19 epithelial cells 2 days postinfection. Average genomes per IU from 3 independent sets of virus stock are plotted, with error bars representing SD. ND, not determined (undetectable levels of infectivity). Asterisks indicate *P* values of ≤ 0.05 , determined by one-way analysis of variance (ANOVA) with Dunnett's multiple-comparison test comparing each recombinant to the parent in three independent experiments.

infection for all recombinants to a range of 30- to 300-fold (Fig. 2B). These results suggested that for the more gH/gL/gO-rich TR and MT, gO polymorphisms may differentially influence the infection of fibroblasts and epithelial cells, shifting the apparent relative tropism. However, such influences were less pronounced for ME, consistent with the low abundance of gH/gL/gO expressed by this virus.

It was not clear if the observed differences in tropism ratios were due to enhanced infection of one cell type, reduced infection of the other cell type, or a mixture of the two. To address this, specific infectivity (ratio of the number of virions to the number of infectious units) was determined for each parent and recombinant on both fibroblasts and epithelial cells. Multiple independent supernatant stocks of each recombinant were analyzed by quantitative PCR (qPCR) for encapsidated viral genomes, and infectious titers on both cell types were determined by flow cytometry quantification of GFP-positive cells (Fig. 3). For the TR-based viruses on fibroblasts, MEGO(GT5), TBGO(GT1c), and TNGO(GT4) each resulted in moderately enhanced infectivity (2- to 10-fold fewer genomes per infectious unit [IU]) compared to the parental TR, and PHGO(GT2a) enhanced infectivity 30-fold. In contrast, ADGO(GT1a) dropped TR infectivity below the detection limit of the flow cytometry-based assay (Fig. 3A, top). In our previous study, expression of MEGO in the TR background did not appear to affect infectivity on fibroblasts (48). This discrepancy was likely due to the more sensitive flow cytometry readout used in the current studies than the plaque assay readout used previously. The infectivity of parental TR on epithelial cells was about 20-fold lower than on fibroblasts (i.e., 20-fold-higher count of genomes per IU), but the relative effect of each heterologous gO was similar to that observed on fibroblasts (Fig. 3A, bottom).

Thus, some of the gO changes had dramatic effects on the infectivity of TR. Although these effects were manifest on both cell types, they were more pronounced on fibroblasts, and this explains the observed differences in fibroblast preferences illustrated in Fig. 2A.

The infectivity of cell-free ME virions on both cell types was below the detection limit of the flow cytometry-based assay, and none of the changes to gO rescued infectivity (Fig. 3B). These results indicated that the cell-free virions of all of the ME-based viruses were virtually noninfectious. When virus was propagated as MT, infectivity on both cell types was improved to levels comparable to those with TR, and this was consistent with our previous results (Fig. 2C) (26, 48). The only significant effect of gO changes on MT occurred with ADgO(GT1a), which reduced infectivity on both cell types. Thus, as in the TR background, some changes to gO influenced infectivity of MT, and this was disproportionately manifest on fibroblasts compared to epithelial cells, but the overall preference of all of the MT-based viruses was strongly in favor of fibroblasts. In contrast, gO changes had little effect on the infectivity or tropism of ME-based viruses.

It has been reported that gO-null HCMV are impaired for attachment to cells and that soluble gH/gL/gO can block HCMV attachment (33, 54). Thus, it was possible that the observed changes to cell-free infectivity due to gO polymorphisms were related to a role for gO in attachment. To test this hypothesis, each heterologous gO recombinant was compared to the corresponding parental strain by applying cell-free virus stocks to fibroblast or epithelial cell cultures for approximately 20 min, washing away the unbound virus, and then counting the cell-associated virions by immunofluorescence staining of the capsid-associated tegument protein pp150 (33) (Fig. 4 and Tables 2 and 3). Given the short incubation time, high concentrations of input viruses were used, and these inputs were equal for each set of parents and heterologous gO recombinants within the constraints of the stock concentrations. Higher inputs were required for ME to obtain detectable numbers of bound virus, consistent with the small amounts of gH/gL/gO in these virions. The average number of cell-associated virions per cell varied considerably between experiments, likely reflecting the complex parameters expected to influence virus attachment, including stock concentration, cell state, and variability in the incubation time between experiments. In some cases, a given recombinant was significantly different from the parent in only one or two of the three experiments. It was concluded that these specific gO isoforms did not affect binding or attachment of HCMV to cells. However, binding of TR_TNgO(GT4) and MT_ADgO(GT1a) were each significantly lower than those of their respective parental viruses in all three experiments on both fibroblasts and epithelial cells. While it was possible that the reduced binding of MT_ADgO(GT1a) was due in part to the slightly smaller amounts of gH/gL/gO (Fig. 1C and Table 1), the reduced binding of TR_TNgO(GT4) could not be similarly explained since this virus had slightly more gH/gL/gO than the parental TR (Fig. 1A and Table 1). Moreover, reduced binding may help explain the lower infectivity of MT_ADgO(GT1a) (Fig. 3C), but the poor infectivity of TR_ADgO(GT1a) could not be explained by poor binding, and the reduced binding of TR_TNgO(GT4) did not result in reduction of infectivity (Fig. 3A).

In sum, these analyses indicated the following. (i) gO polymorphisms can influence the cell-free infectivity of HCMV. In some cases this was independent of any effects on abundance of gH/gL/gO in the virion envelope or binding to cells [e.g., parental TR and TR recombinants harboring MEgO(GT5), TBgO(GT1c), and ADgO(GT1a) had dramatically different infectivities but comparable levels of gH/gL/gO and cell binding]. (ii) The influence of some gO isoforms was dependent on the background strain [e.g., PHgO(GT2a) enhanced TR infectivity but did not affect ME or MT and TNgO(GT4) reduced binding of TR but had no effect on binding of ME or MT]. (iii) While some heterologous gO recombinants had quantitatively different effects on infectivity on fibroblasts versus epithelial cells, these did not change the fundamental fibroblast preferences for either TR or MT. (iv) Some of the heterologous gOs did appear to change relative tropism of ME. However, the relevance of tropism ratios for these

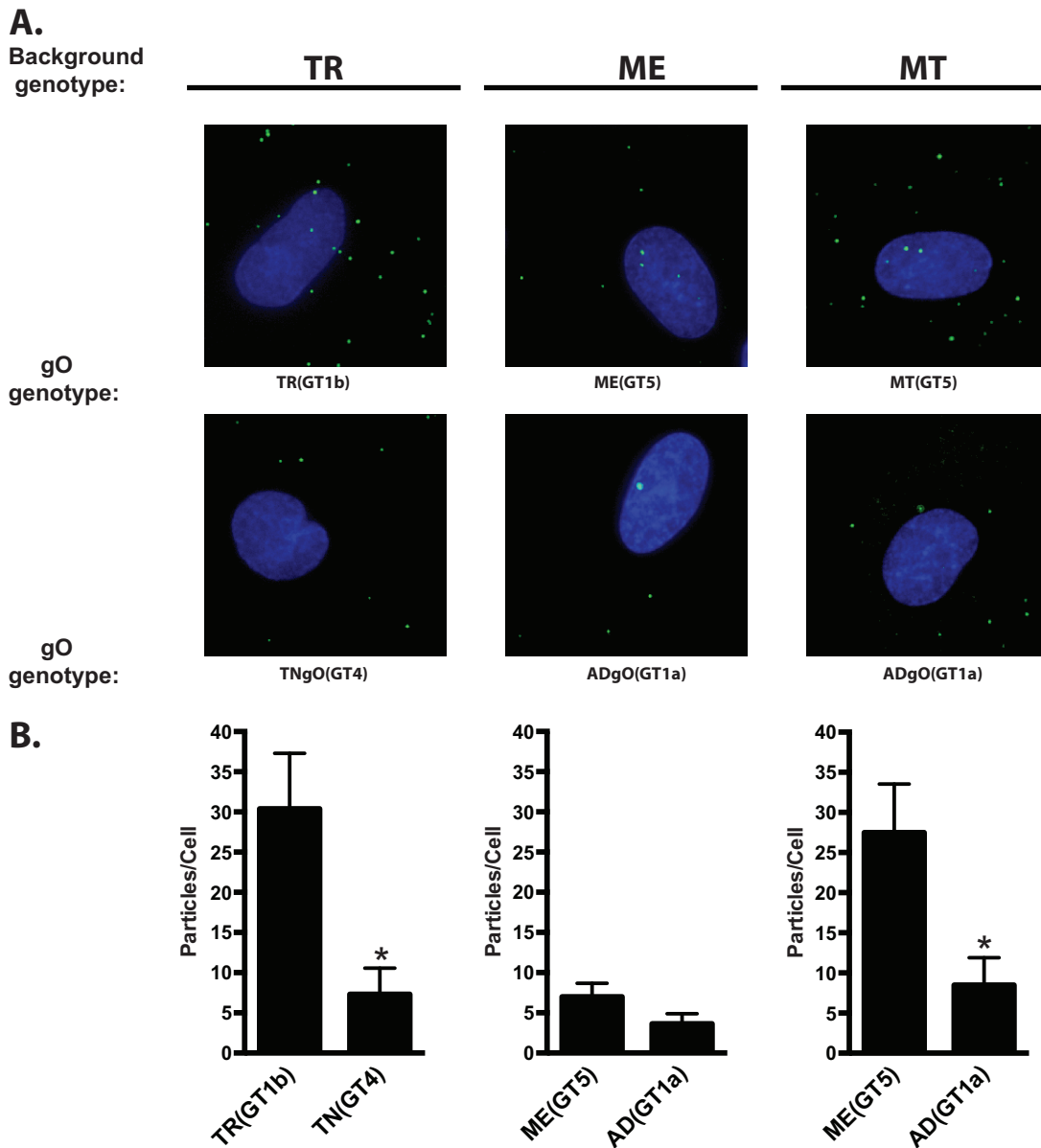


FIG 4 Binding of parental and heterologous gO recombinant HCMV to fibroblasts. Extracellular HCMV TR, ME, or MT or the corresponding heterologous gO recombinants were applied to nHDF for 20 min. Multiplicities (genomes/cell) were as follows: TR background viruses, 1×10^4 ; ME background viruses, 5×10^4 ; and MT background viruses, 1×10^4 . After unbound virus was washed away, cultures were fixed and permeabilized with acetone and cell-associated virus particles were detected by immunofluorescence using antibodies specific for the capsid-associated tegument protein pp150. Cells were visualized by staining nuclei with DAPI. (A) Representative fields of parental TR, ME, and MT and heterologous gO recombinants that consistently reduced binding in 3 independent experiments (Table 2). (B) Mean particles per cell for representative experiments. Error bars represent SD. Asterisks indicate P values of ≤ 0.05 , determined by one-way ANOVA with Dunnett's multiple-comparison test comparing each recombinant to the parent.

viruses is questionable since the specific infectivity (genomes per IU) analyses suggested that all ME-based recombinants were noninfectious on either cell type. This was consistent with the highly cell-associated nature of ME (50, 51).

Polymorphisms in gO can differentially influence the mechanisms of cell-free and cell-to-cell spread. The analyses described above focused on the cell-free infectivity of HCMV, as indicative of a cell-free mode of spread. Cell-to-cell spread mechanisms are likely important for HCMV, and while gH/gL complexes are clearly important for cell-to-cell spread, the mechanisms in these processes are poorly characterized in comparison to the case with cell-free infection. Strains TR and ME are well suited to

TABLE 2 Binding of parental and heterologous gO recombinant HCMV to fibroblasts

Virus	Expt 1 ^a			Expt 2 ^b			Expt 3 ^c		
	Mean ^d	Fold ^e	ANOVA ^f	Mean	Fold	ANOVA	Mean	Fold	ANOVA
TR_TR(GT1b)	17.8	—	—	31.2	—	—	30.4	—	—
TR_MEgO(GT5)	21.2	—	NS	44.7	1.4	*	37.9	—	NS
TR_PHgO(GT2a)	24.3	—	NS	12.7	0.41	*	35.3	—	NS
TR_TBgO(GT1c)	18.8	—	NS	30.5	—	NS	33.7	—	NS
TR_ADgO(GT1a)	25.7	—	NS	24.7	—	NS	23.3	—	NS
TR_TNgO(GT4)^g	4.9	0.27	*	6.9	0.22	*	7.3	0.24	*
ME_MEgO(GT5)	21.6	—	—	5.8	—	—	7	—	—
ME_TR(GT1b)	5.3	0.25	*	7.1	—	NS	3.9	0.56	*
ME_PHgO(GT2a)	8.0	0.37	*	7.5	—	NS	2.3	0.33	*
ME_TBgO(GT1c)	15.9	0.74	*	9.0	—	NS	7	—	NS
ME_ADgO(GT1a)	2.4	0.11	*	2.4	—	NS	3.7	0.53	*
ME_TNgO(GT4)	5.8	0.27	*	8.5	—	NS	7.4	—	NS
MT_MEgO(GT5)	27.5	—	—	63.9	—	—	120.9	—	—
MT_TR(GT1b)	28.5	—	NS	40.2	0.63	*	159.4	—	NS
MT_PHgO(GT2a)	33.4	—	NS	50.4	—	NS	222	1.84	*
MT_TBgO(GT1c)	44.6	1.6	*	66.2	—	NS	220.8	1.83	*
MT_ADgO(GT1a)	8.5	0.31	*	13.4	0.21	*	23.6	0.2	*
MT_TNgO(GT4)	32.5	—	NS	61.8	—	NS	133.2	—	NS

^aInput concentration of cell-free virus stock (genomes/ml): TR-based viruses, 6.2×10^7 ; ME-based viruses, 2.0×10^8 ; MT-based viruses, 1.0×10^8 .

^bInput concentration of cell-free virus stock (genomes/ml): TR-based viruses, 7.5×10^7 ; ME-based viruses, 5.0×10^8 ; MT-based viruses, 2.0×10^8 .

^cInput concentration of cell-free virus stock (genomes/ml): TR-based viruses, 1.0×10^8 ; ME-based viruses, 5.0×10^8 ; MT-based viruses, 5.0×10^8 .

^dAverage pp150 puncta detected by immunofluorescence per cell in 10 microscopy fields; approximately 4 to 6 cells per field.

^eFold difference in mean pp150 puncta per cell compared to parental virus, determined for recombinant viruses that were significantly different ($P \leq 0.05$) from parental within an experiment. —, value not calculated.

^fOne-way ANOVA with Dunnett's multiple-comparison test comparing each recombinant to the parent. *, $P \leq 0.05$. NS, not significant.

^gBold font indicates recombinant viruses that were significantly different (> or <) in all 3 experiments.

compare the effects of gO polymorphisms on cell-free and cell-to-cell spread since ME is mostly restricted to cell-to-cell due to the poor infectivity of cell-free virions but can be allowed to also spread cell-free by propagation as MT, whereas TR can spread by both cell-free and cell-to-cell mechanisms (23, 26, 50, 51).

To compare spread among heterologous gO recombinants, replicate cultures were infected at low multiplicity, and at 12 days postinfection (dpi), focus morphology was documented by fluorescence microscopy and the increased number of infected cells was determined by flow cytometry. In fibroblast cultures, parental TR and MT produced larger, more diffuse foci whereas parental ME produced smaller, more tightly localized foci (Fig. 5A). These focal patterns were consistent with the notion that TR and MT spread by both cell-free and cell-to-cell mechanisms, but that ME was restricted to cell-to-cell spread. Quantitatively, spread by parental TR increased the numbers of infected cells 55-fold over 12 days, whereas spread of TR_MEgO(GT5) and TR_PHgO(GT2a) was significantly reduced (Fig. 5B). Spread of ME was slightly reduced by ADgO(GT1a) but was increased by TNgO(GT4) (Fig. 5C). Surprisingly, different effects on spread were observed for MT: TBgO(GT1c) and TNgO(GT4) reduced spread, and ADgO(GT1a) increased spread.

A number of interesting incongruities were observed when comparing the cell-free infectivity of some gO recombinants on fibroblasts to their respective spread characteristics in fibroblasts. (i) Spread of TR_PHgO in fibroblasts was reduced compared to that of the parental TR (Fig. 5B), but the cell-free infectivity of this recombinant was actually better (Fig. 3A). Similarly, spread of both MT_TBgO(GT1c) and MT_TNgO(GT4) was reduced in fibroblasts (Fig. 5D), but cell-free infectivity of both viruses was comparable to that of parental MT. (ii) Conversely, MT_ADgO(GT1a) spread better in fibroblasts (Fig. 5D), but the cell-free infectivity was substantially worse (Fig. 3C). Since the efficiency of cell-free spread should depend on both the specific infectivity and the quantities of progeny virus released to the culture supernatants, it was possible that some of these incongruities reflected offsetting differences in the quantity of cell-free virus released compared to their infectivity. To test this, progenies released from infected fibroblasts into culture supernatants were quantified by qPCR. There were no

TABLE 3 Binding of parental and heterologous gO recombinant HCMV to epithelial cells

Genotype background	Expt 1 ^a			Expt 2 ^b			Expt 3 ^c		
	Mean ^d	Fold ^e	ANOVA ^f	Mean	Fold	ANOVA	Mean	Fold	ANOVA
TR_TR(GT1b)	26.2	—	—	41.7	—	—	43.7	—	—
TR_MEgO(GT5)	35.5	1.35	*	38.3	—	NS	56.8	—	NS
TR_PHgO(GT2a)	33.4	—	NS	19.3	0.46	*	61	1.4	*
TR_TBgO(GT1c)	24.1	—	NS	35.4	—	NS	58.7	1.34	*
TR_ADgO(GT1a)	36.4	1.39	*	22.2	0.53	*	36	—	NS
TR_TNgO(GT4)^g	16.2	0.62	*	18.62	0.45	*	23.4	0.54	*
ME_MEgO(GT5)	37.3	—	—	18	—	—	15	—	—
ME_TR(GT1b)	17.7	0.47	*	24.9	—	NS	10.4	0.69	*
ME_PHgO(GT2a)	22.3	0.6	*	23	—	NS	9.4	0.62	*
ME_TBgO(GT1c)	34.1	—	NS	32.3	1.79	*	18.6	—	NS
ME_ADgO(GT1a)	14.4	0.39	*	11.4	—	NS	10.8	0.72	*
ME_TNgO(GT4)	24.4	0.65	*	25.9	1.44	*	14.3	—	NS
MT_MEgO(GT5)	33.2	—	—	68	—	—	236.8	—	—
MT_TRgO(GT1b)	35.3	—	NS	46.1	0.68	*	210.1	—	NS
MT_PHgO(GT2a)	46.5	—	NS	78	—	NS	383.2	1.62	*
MT_TBgO(GT1c)	63.4	1.91	*	69.6	—	NS	238.3	—	NS
MT_ADgO(GT1a)	16.7	0.5	*	26.1	0.38	*	26.6	0.11	*
MT_TNgO(GT4)	44.1	—	NS	48.1	0.71	*	150.9	0.64	*

^aInput concentration of cell-free virus stock (genomes/ml): TR-based viruses, 6.2×10^7 ; ME-based viruses, 2.0×10^8 ; MT-based viruses, 1.0×10^8 .

^bInput concentration of cell-free virus stock (genomes/ml): TR-based viruses, 7.5×10^7 ; ME-based viruses, 5.0×10^8 ; MT-based viruses, 2.0×10^8 .

^cInput concentration of cell-free virus stock (genomes/ml): TR-based viruses, 1.0×10^8 ; ME-based viruses, 5.0×10^8 ; MT-based viruses, 5.0×10^8 .

^dAverage pp150 puncta detected by immunofluorescence per cell in 10 microscopy fields; approximately 4 to 6 cells per field.

^eFold difference in mean pp150 puncta per cell compared to parental virus, determined for recombinant viruses that were significantly different ($P \leq 0.05$) from the parent within an experiment. —, value not calculated.

^fOne-way ANOVA with Dunnett's multiple-comparison test comparing each recombinant to the parent. *, $P \leq 0.05$. NS, not significant.

^gBold font indicates recombinant viruses that were significantly different from the parent in the same direction (> or <) in all 3 experiments.

significant differences in the quantity of progeny released per cell for any of the TR- or ME-based recombinants (Fig. 6A and B). Likewise, all of the MT-based recombinants released similar numbers of cell-free progeny except for MT_ADgO(GT1a), which was reduced by approximately 4-fold (Fig. 6C). Thus, the discrepancies between efficiency of spread and cell-free infectivity could not be explained by offsetting differences in the release of cell-free progeny. Rather, these results suggested that gO polymorphisms can differentially influence the mechanisms of cell-free and cell-to-cell spread in fibroblasts. The interpretation that gH/gL/gO can provide a specific function for cell-to-cell spread was supported by the results showing that expression of ADgO(GT1a) and TNgO(GT4), respectively, reduced and increased spread of the strain ME, for which spread is almost exclusively cell to cell (Fig. 5C).

Spread was also analyzed in epithelial cell cultures. Foci of both TR and ME remained tightly localized, suggesting predominantly cell-to-cell modes of spread for both strains in this cell type (Fig. 7A). The number of TR-infected cells increased only 5- to 6-fold over 12 days, compared to approximately 25-fold for ME (Fig. 7B and C). The low efficiency of spread for TR in epithelial cells compared to that of ME was documented previously and may relate to the low expression of gH/gL/UL128-131 by TR compared to that by ME (23, 26, 55). Expression of TNgO(GT4) further reduced TR spread in epithelial cells (Fig. 7B). In contrast, ME spread was slightly reduced by TBgO(GT1c) and ADgO(GT1a) but nearly doubled by TNgO(GT4). The observed increase in ME spread due to TNgO(GT4) was not attributed to increased release of progeny to the culture supernatants in epithelial cells (Fig. 8). Note that spread of MT could not be addressed in epithelial cells, since gH/gL/UL128-131 is clearly required for spread in these cells and its repression would complicate analysis of the contribution of gO polymorphisms (23). Nevertheless, it is clear from these experiments that gO polymorphisms can affect spread in epithelial cells and that this can depend on the background strain. Specifically, TNgO(GT4) reduced TR spread but increased ME spread. This suggested that although gH/gL/UL128-131 is required for efficient cell-to-cell spread in epithelial cells and may even be sufficient in the case of gO-null HCMV (25, 27), gH/gL/gO may also contribute to the mechanism when present.

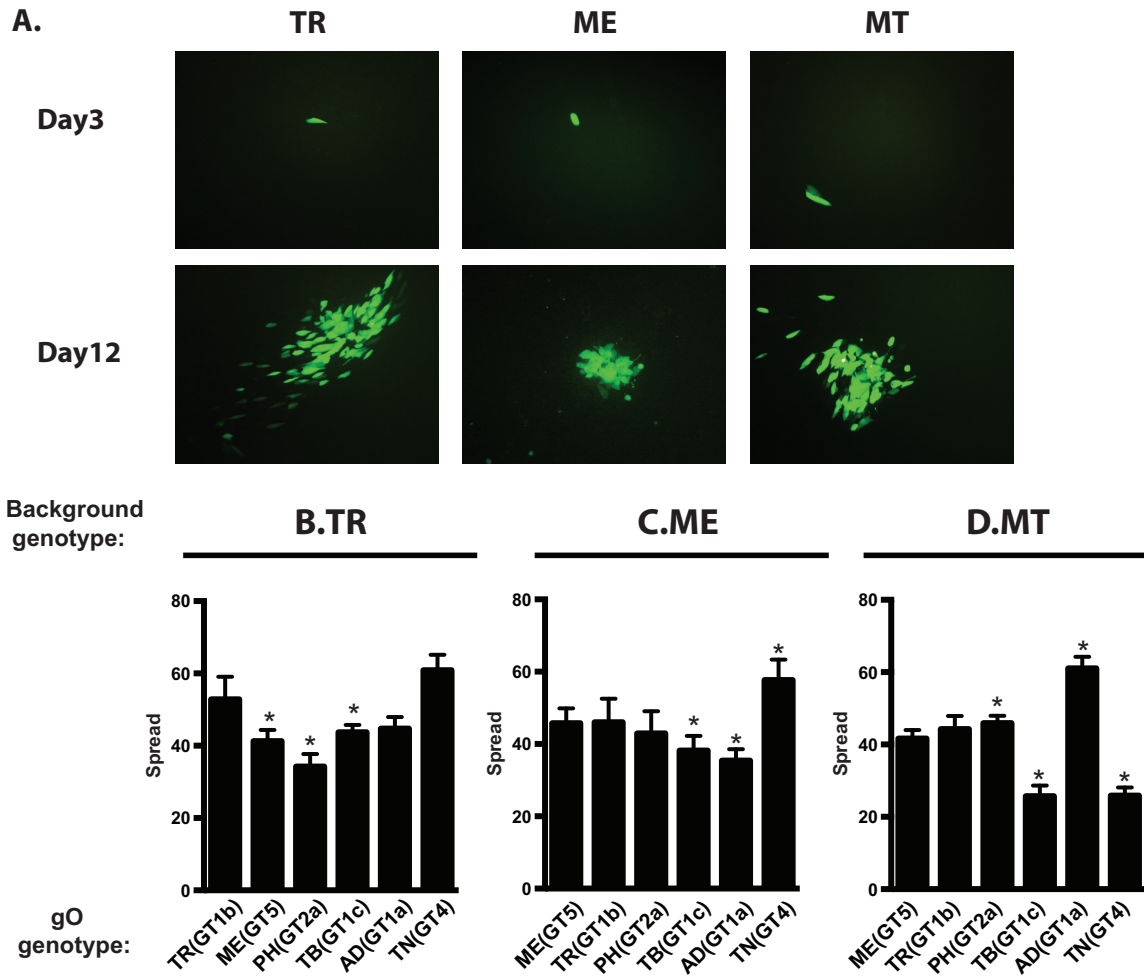


FIG 5 Spread of parental and heterologous gO recombinant HCMV in fibroblast cultures. Confluent monolayers of nHDF or HFFFTet (for MT) were infected with 0.003/cell of HCMV TR (A and B), ME (A and C), or MT (A and D) or the corresponding heterologous gO recombinants. At 3 and 12 days postinfection, cultures were analyzed by fluorescence microscopy (A) or by flow cytometry to quantitate the total number of infected (GFP⁺) cells (B to D). Plotted are the average numbers of infected cells at day 12 per infected cell at day 3 in 3 independent experiments. Error bars represent SD. Asterisks indicate *P* values of ≤ 0.05 , determined by one-way ANOVA with Dunnett's multiple-comparison test comparing each recombinant to the parent.

Polymorphisms in gO can affect antibody neutralization on gH epitopes. The extensive N-linked glycosylation of gO raised the possibility that gO could present steric hindrance to the binding of antibodies to epitopes on gH/gL, as was shown for HCMV gN and also HIV Env (44, 45). A corollary hypothesis was that such effects might vary with the polymorphisms among gO isoforms. To address this, neutralization experiments were conducted using two anti-gH monoclonal antibodies (MAbs): 14-4b, which recognizes a discontinuous epitope likely located near the membrane-proximal ectodomain of gH (35, 56), and AP86, which binds to a continuous epitope near the N terminus of gH (57). Note that these experiments could only be performed with TR- and MT-based recombinants since the cell-free progenies of ME-based viruses were found to be only marginally infectious (Fig. 3B).

Parental TR and recombinants encoding MEgO(GT5), PHgO(GT2a), and TBgO(GT1c) were completely neutralized on fibroblasts by MAb 14-4b, whereas TR_ADgO(GT1a) and TR_TNgO(GT4) were significantly resistant (Fig. 9A). There was more variability among TR-based recombinants with MAb AP86 (Fig. 9B). In this case, parental TR could be neutralized only to approximately 40% residual infection. TNgO(GT4) rendered TR totally resistant to MAb AP86, and MEgO(GT5) also significantly protected TR. In contrast, TR_TBgO(GT1c) and TR_ADgO(GT1a) were more sensitive to MAb AP86. On

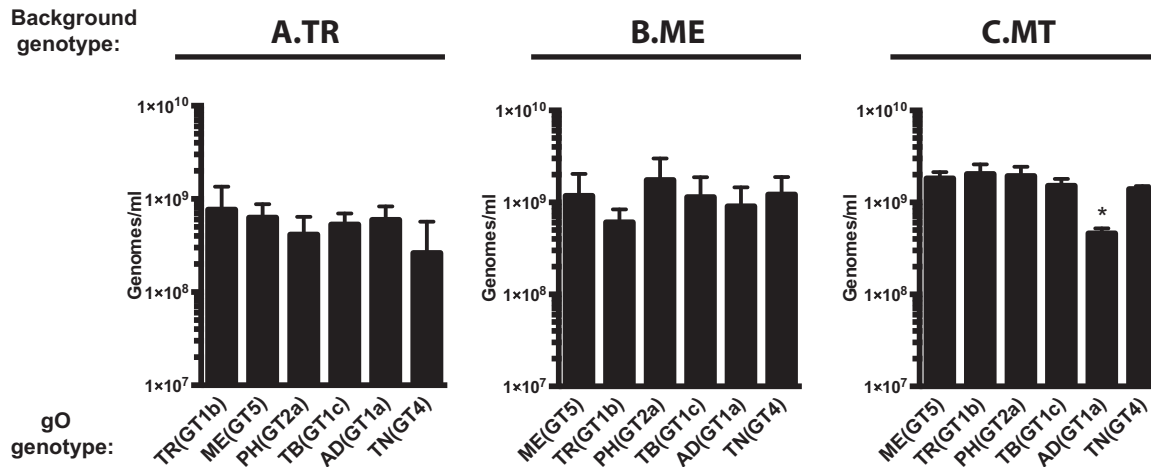


FIG 6 Release of extracellular progeny by parental and heterologous gO recombinant HCMV in fibroblast cultures. Cultures of nHDF or HFFFTet (for MT) were infected with 1 IU/cell of HCMV TR (A), ME (B), or MT (C) or the corresponding heterologous gO recombinants for 8 days. The number of infected cells was determined by flow cytometry, and progeny virus in culture supernatants was quantified by qPCR for viral genomes. The average number of extracellular virions per milliliter in each of 3 independent experiments is plotted. Error bars represent SD. Asterisks indicate *P* values of ≤ 0.05 , determined by one-way ANOVA with Dunnett's multiple-comparison test comparing each recombinant to the parent.

epithelial cells, neutralization by both antibodies was more potent and complete than on fibroblasts, and there was less variability among gO recombinants (Fig. 9C and D). This was consistent with the interpretation that both 14-4b and AP86 could bind their epitopes on gH/gL/UL128-131 and that this represented the majority of the observed neutralization on epithelial cells. However, TR_TNgO(GT4) still displayed some reduced sensitivity to both antibodies, suggesting that gH/gL/gO epitopes also contributed to neutralization on epithelial cells.

MT-based recombinants were generally more sensitive to neutralization by 14-4b than were TR-based viruses (compare 14-4b concentrations in Fig. 9A and 10A). Strikingly, whereas TNgO(GT4) conferred 14-4b resistance to TR, it did not in MT, and instead ADgO(GT1a) provided resistance to 14-4b (Fig. 10A). As was observed for TR-based recombinants, 14-4b neutralization on epithelial cells was less affected by gO polymorphisms (Fig. 10B). Note that neutralization of MT-based recombinants by AP86 could not be tested since MEgH harbors a polymorphism in the linear AP86 epitope that precludes reactivity (57). Together, these results indicated that differences among gO genotypes can differentially affect antibody neutralization on gH epitopes. Moreover, which gO genotype could protect against which antibody depended on the background strain, suggesting the combined effects of gO polymorphisms and gH/gL polymorphisms.

DISCUSSION

Efficient cell-free infection of most, if not all, cell types requires gH/gL/gO (22, 25, 26). However, the details of the mechanisms, and the distinctions between the roles of gH/gL/gO in cell-free and cell-to-cell spread, remain to be clarified. While there are naturally occurring amino acid polymorphisms in each subunit of gH/gL/gO, gO has the most dramatic variation, with 8 known genotypes (or alleles) that differ between 10 and 30% of amino acids (9–12). All isoforms of gO are predicted to have extensive N-linked glycan modifications, and some of the amino acid differences alter the predicted sites. In a previous study, we sought to determine if gO polymorphisms were a factor influencing the different levels of gH/gL/gO and gH/gL/UL128-131 in strains TR and ME. On the contrary, results suggested that genetic differences outside the UL74(gO) ORF result in more rapid degradation of gO in the ME-infected cells than with TR, and this influences the pool of gO available during progeny assembly (48). Kalsner et al. reported that gO polymorphisms could differentially affect multistep replication kinetics in

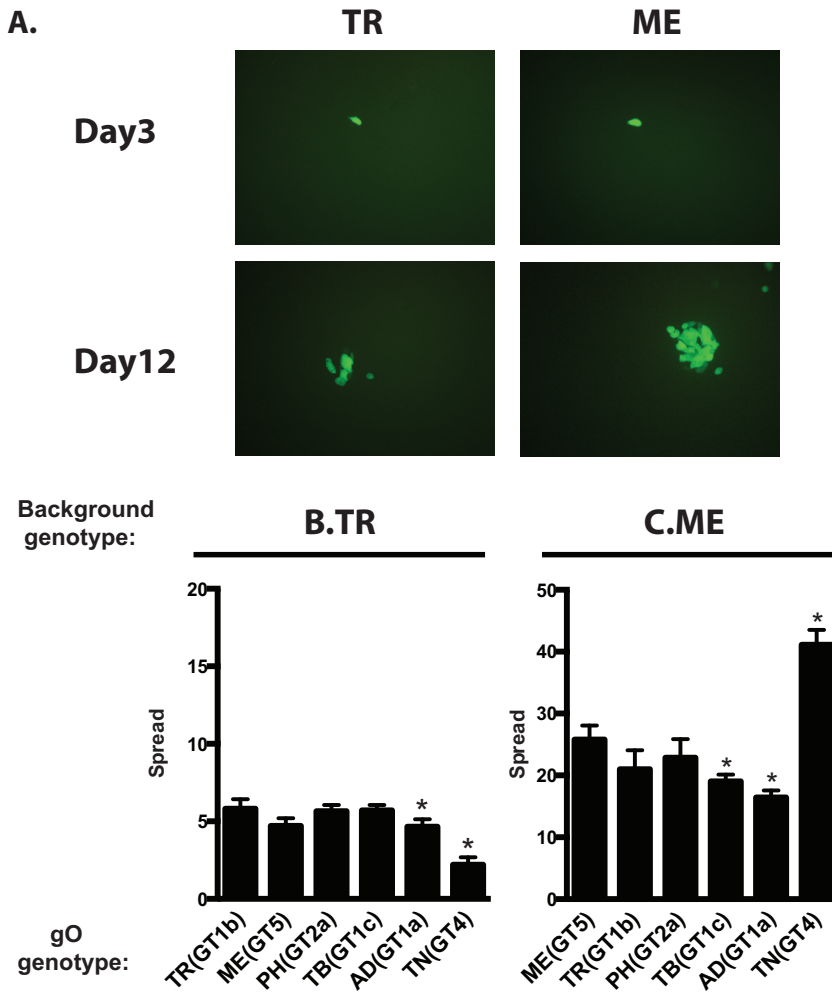


FIG 7 Spread of parental and heterologous gO recombinant HCMV in epithelial cell cultures. Confluent monolayers of ARPE19 cells were infected with 0.003 IU/cell of HCMV TR (A, B), ME (A, C), or the corresponding heterologous gO recombinants. At 3 and 12 days postinfection, cultures were analyzed by fluorescence microscopy (A) or by flow cytometry to quantitate the total number of infected (GFP⁺) cells (B and C). Plotted are the average numbers of infected cells at day 12 per infected cell at day 3 in 3 independent experiments. Error bars represent SD. Asterisks indicate *P* values of ≤ 0.05 , determined by one-way ANOVA with Dunnett’s multiple-comparison test comparing each recombinant to the parent.

fibroblasts and epithelial cells (49). However, only TB was analyzed, as the background and distinctions between effects on cell-free and cell-to-cell spread were unclear. In this study, we constructed a matched set of heterologous gO recombinants in the well-characterized, BAC-cloned strains TR and ME. Studies included address aspects of cell-free and cell-to-cell spread, cell type tropism, and neutralization by anti-gH antibodies. The results demonstrate that gO polymorphisms can influence each of these parameters, and the effects in some cases were dependent on the genetic background, suggesting a number of possible epistatic phenomena at play.

A commonly used measure to assess the tropism of HCMV strains, isolates, and recombinants is the ratio of infection between fibroblasts and other cell types, including epithelial and endothelial cells (49, 55, 58, 59). Expressions of this ratio have varied but have generally involved a normalization of the epithelial or endothelial infection to that of fibroblasts. In this study, we similarly determined the infectious titer of each of the parental strains and heterologous gO recombinants on both fibroblasts and epithelial cells and expressed ratios ≥ 1 (either fibroblasts/epithelial or epithelial/fibroblasts) to indicate the fold cell type preference or tropism of each virus (Fig. 2). Both gH/gL/gO-rich viruses, TR and MT, were strongly fibroblast tropic, and some heterolo-

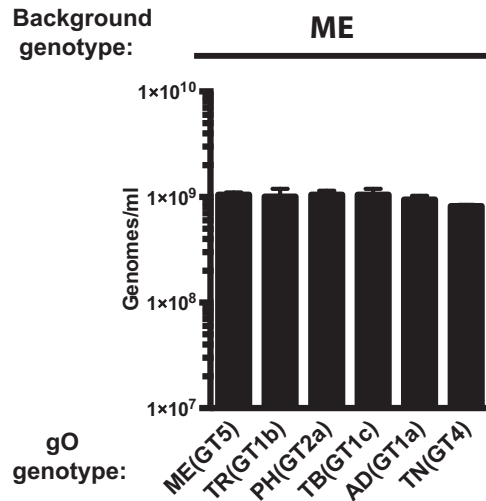
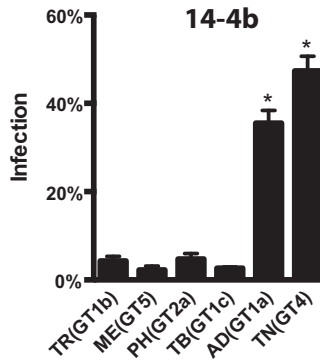
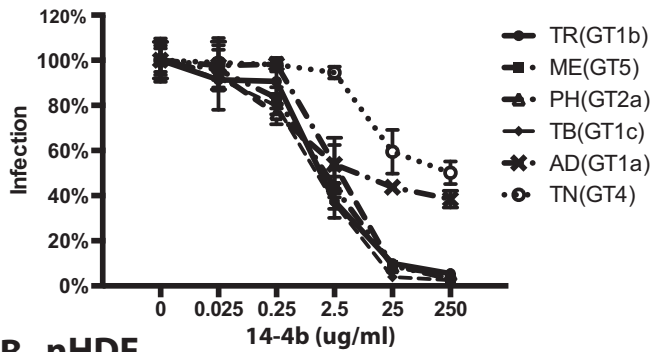


FIG 8 Release of extracellular progeny by parental and heterologous gO recombinant HCMV ME in epithelial cell cultures. Cultures of ARPE19 epithelial cells were infected with HFFtet-derived MT or corresponding heterologous gO recombinants at the highest multiplicities possible given the specific infectivity of stocks reported in Fig. 3 (approximately 0.0005 IU/cell). (Note that since APRE19 cells do not express TetR, after the initial infection, MT replicates as ME). Cultures were then propagated by trypsinization and reseeding of intact cells until the number of infected cells approached 90 to 100% by microscopic inspection for GFP⁺ cells. After 8 more days, culture supernatants were then analyzed by qPCR for viral genomes. The average number of extracellular virions per ml in each of 3 independent experiments is plotted. Error bars represent SD. Asterisks indicate *P* values of ≤ 0.05 , determined by one-way ANOVA with Dunnett's multiple-comparison test comparing each recombinant to the parent.

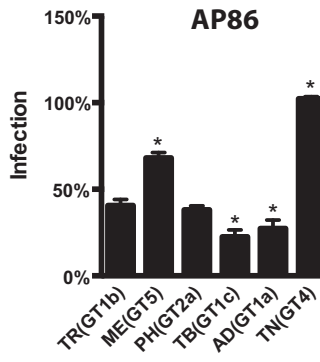
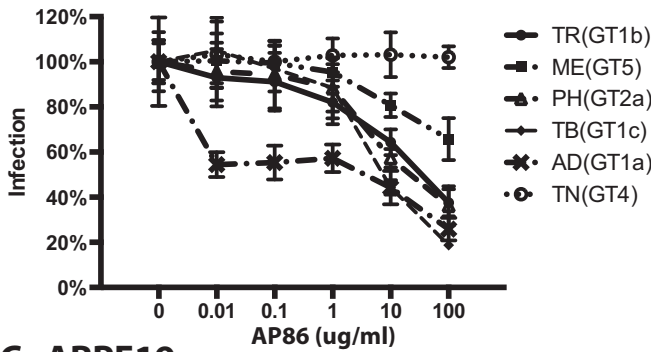
gous gO isoforms enhanced this preference, while others reduced it. In contrast, the gH/gL/UL128-131-rich virus ME infected both cell types more equally (ratios closer to 1), and gO polymorphisms had little effect. The limitation of any such measure of relative tropism is that it does not determine whether the virus in question can efficiently infect one cell type in particular, both, or neither. Thus, any 2 viruses compared may have the same fibroblast-to-epithelial cell infectivity ratio for completely different reasons. To address this, we also compared infectivities on the two cell types using a common comparison for all viruses, i.e., the number of virions in the stock as determined by qPCR for DNase-protected viral genomes in the cell-free virus stocks (Fig. 3). This analysis provided a measure of specific infectivity as the number of genomes per IU, where the lower ratio indicates more efficient infection. Whether higher values for genome per IU reflect the presence of greater numbers of bona fide "defective" virions or a lower probability or efficiency of each viable virion in the stock to accomplish a detectable infection, and whether or how these two possibilities are different, is difficult to know for any type of virus. Nevertheless, these analyses provided important insights to the tropism ratios reported. In general, the specific infectivity ratios of the gH/gL/gO-rich viruses TR and MT in these experiments were in the range of 500 to 5,000 genomes/IU on fibroblasts, but these viruses were approximately 20- to 100-fold less infectious on epithelial cells, explaining the strong fibroblast preference exhibited by these strains. The effects of most heterologous gO isoforms were similar on both cell types but often of larger magnitude on fibroblasts. Thus, while all of the TR- and MT-based gO recombinants remained fibroblast tropic, the quantitatively different effects on the two cell types influenced the magnitude of fibroblast preference. Importantly, in no case did the change of gO affect the fundamental fibroblast preference of either TR or MT. The infectivity of the gH/gL/UL128-131-rich, ME-based viruses on both cell types was undetectable in these assays. Thus, the near neutral fibroblast-to-epithelial cell tropism ratios of the ME-based viruses seem to reflect equal inability to infect these cell types, and any assertion of a "preference" for either cell type for extracellular ME virions seems spurious.

Binding to PDGFR α through gO is clearly critical for infection of fibroblasts (30).

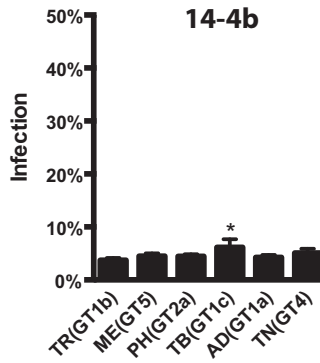
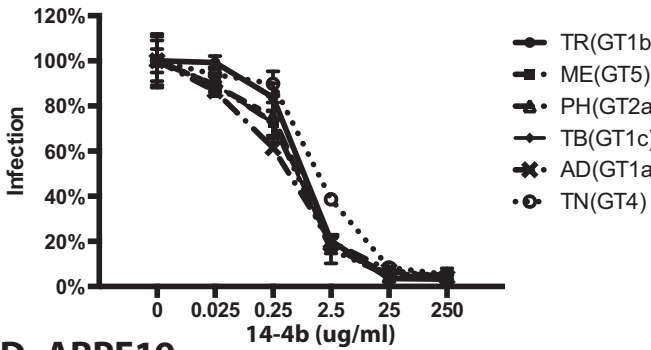
A. nHDF



B. nHDF



C. ARPE19



D. ARPE19

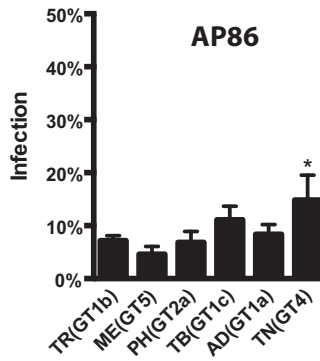
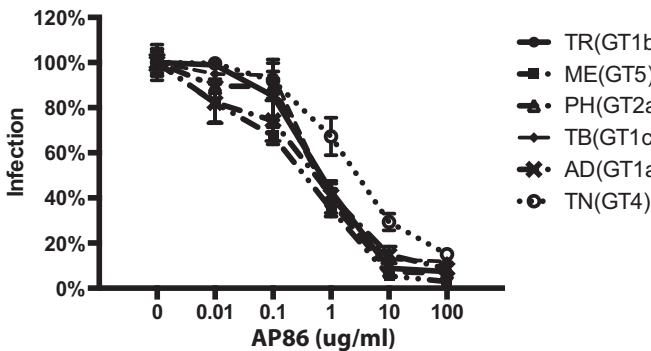


FIG 9 Neutralization of parental HCMV TR and heterologous gO recombinant by anti-gH antibodies. Genome equivalents of extracellular HCMV TR or the corresponding heterologous gO recombinants were incubated with 0.025 to 250 μ g/ml of anti-gH MAb 14-4b or 0.01 to 100 μ g/ml of anti-gH MAb AP86 and then plated on cultures of nHDF (A and B) or ARPE19 epithelial cells (C and D). At 2 days postinfection, the number of infected (GFP⁺) cells was determined by flow cytometry and plotted as the percentage of the no-antibody control. (Left graphs) Full titration curves shown are representative of results from three independent experiments, each performed in triplicate. (Right graphs) Average percent of cells infected at the highest antibody concentrations in 3 independent experiments. Error bars represent SD. Asterisks indicate *P* values of ≤ 0.05 , determined by one-way ANOVA with Dunnett's multiple-comparison test comparing each recombinant to the parent.

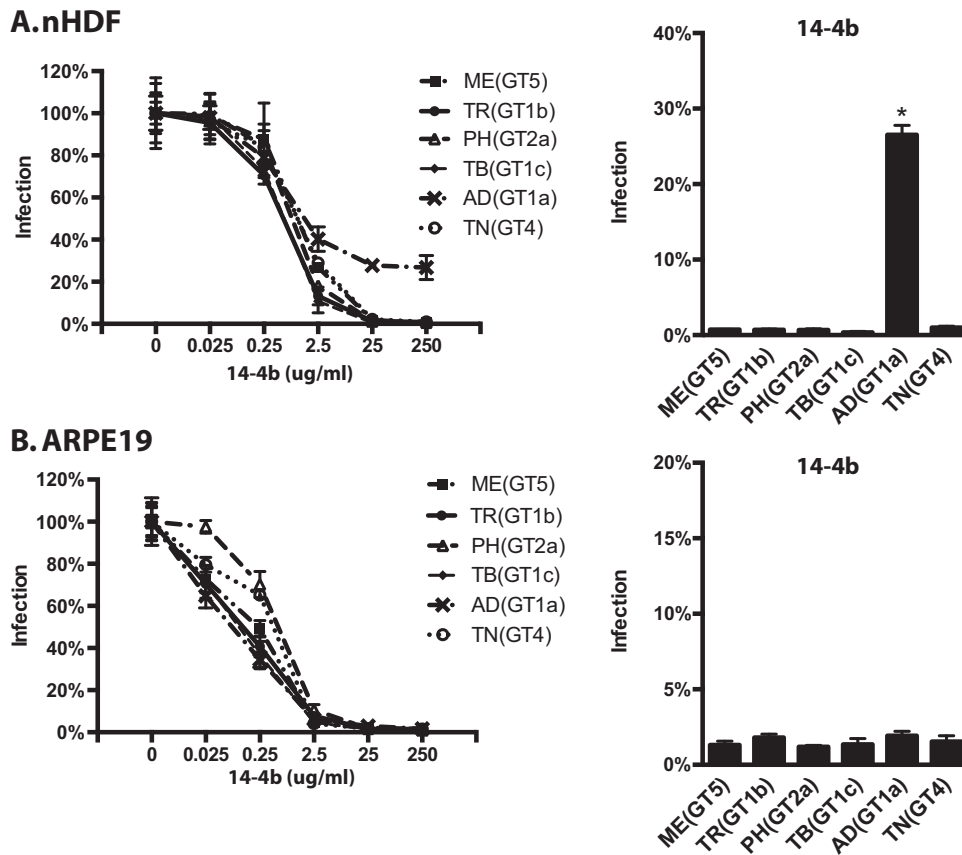


FIG 10 Neutralization of parental HCMV MT and heterologous gO recombinant by anti-gH antibodies. Genome equivalents of extracellular HCMV MT or the corresponding heterologous gO recombinants were incubated with 0.025 to 250 µg/ml of anti-gH MAb 14-4b and then plated on cultures of nHDF (A) or ARPE19 epithelial cells (B). At 2 days postinfection, the number of infected (GFP⁺) cells was determined by flow cytometry and plotted as the percentage of the no-antibody control. (Left graphs) Full titration curves shown are representative of three independent experiments, each performed in triplicate. (Right graphs) Average percent of cells infected at the highest antibody concentrations in 3 independent experiments. Error bars represent SD. Asterisks indicate *P* values of ≤ 0.05 , determined by one-way ANOVA with Dunnett's multiple-comparison test comparing each recombinant to the parent.

However, while gH/gL/gO is also important for infection of epithelial cells, the literature is conflicted on the expression of PDGFR α and its importance for HCMV infection in epithelial and endothelial cells (26, 28, 29, 32, 33). On either cell type, possible mechanisms of gH/gL/gO include facilitating initial attachment to cells, promoting gB-mediated membrane fusion, and signaling through PDGFR α or other receptors. While Wu et al. were able to coimmunoprecipitate gB with gH/gL/gO and PDGFR α , Vanarsdall et al. showed that gH/gL without gO or UL128-131 can directly interact with gB and promote gB fusion activity (20, 32, 34). It has also been shown that gH/gL/gO engagement of PDGFR α can elicit signaling cascades but that this is not required for infection (28, 30, 32). In contrast, there is evidence that gH/gL/gO can help facilitate initial virion attachment (33, 54). In our studies, TNgO(GT4) reduced binding of TR to both fibroblasts and epithelial cells (Fig. 4 and Tables 2 and 3). However, the reduced binding of TR_TNgO(GT4) did not result in reduced infection of either cell type, and there were other isoforms of gO that resulted in either increased or decreased infectivity but were not associated with any detectable alteration in binding. Thus, while gH/gL/gO may contribute to initial binding, it is likely involved in other important mechanisms that facilitate infection and these can be influenced by gO polymorphisms. For example, it is possible that polymorphisms in gO can affect the nature and outcome of PDGFR α engagement. In support of this hypothesis, Stegmann et al. showed that mutation of conserved residues within the N-terminal variable domain of gO were

critical for PDGFR α binding (60). Thus, it is conceivable that the variable residues of gO can alter the architecture of the interaction with PDGFR α . Alternatively, it may be that there are other receptors on both cell types for gH/gL/gO and that gO polymorphisms can affect those interactions. Also, the effects of several specific gO isoforms observed in the TR background were not observed in the ME or MT background. Possible explanations for the apparent epistasis include not only the differential contributions of polymorphisms in gH/gL but also potential differences between strains in other envelope glycoproteins, such as gB, or gM/gN may influence the relative importance of gH/gL/gO for binding and infection.

The mechanistic distinctions between cell-free and cell-to-cell spread of HCMV are unclear. Spread of ME in fibroblasts and epithelial and endothelial cells is almost exclusively cell to cell, and this can be at least partially explained by the noninfectious nature of cell-free ME virions (Fig. 3) (27, 50, 51, 55). Laib Sampaio et al. showed that inactivation of the UL74(gO)ORF in ME did not impair spread but that a dual inactivation of both gO and UL128 completely abrogated spread (27). This indicates that gH/gL/UL128-131 is sufficient for cell-to-cell spread in fibroblasts or endothelial cells in the absence of gH/gL/gO, and it seems likely that spread in epithelial cells might be similar in this respect. Our finding that various heterologous gO isoforms can enhance or reduce spread of ME without affecting the cell-free infectivity strongly suggests that while gH/gL/UL128-131 may be sufficient for cell-to-cell spread, gH/gL/gO can modulate or mediate the process if present in sufficient amounts. In the context of MT, where expression of gH/gL/UL128-131 is reduced to subdetectable levels (26, 51), the virus gained cell-free spread capability, and yet some of the heterologous gO isoforms had opposite effects on cell-free infectivity and spread (compare Fig. 3C to Fig. 5D). Similar discordances between cell-free infectivity and spread were observed for the naturally gH/gL/gO-rich strain TR, albeit with different heterologous gO isoforms involved. That gO polymorphisms can have opposite effects on cell-free and cell-to-cell spread supports a hypothesis of mechanistic differences in how gH/gL/gO mediates the two processes, and again these effects seem dependent on epistatic influences of the different genetic backgrounds.

Beyond the roles of gH/gL/gO in replication, the complex is likely a significant target of neutralizing antibodies and therefore a valid candidate for vaccine design. Several groups have reported neutralizing antibodies that react with epitopes contained on the gH/gL base of both gH/gL/UL128-131 and gH/gL/gO and others that react to gO (35–43). We found that changing the gO isoform can have dramatic effects on the sensitivity to two anti-gH MAbs (Fig. 9 and 10). In the TR background on fibroblasts, both ADgO(GT1a) and TNgO(GT4) conferred significant resistance to neutralization by 14-4b, which likely reacts to a discontinuous epitope near the membrane-proximal ectodomain of gH (35, 56). TNgO(GT4) also conferred resistance to AP86, which reacts to a linear epitope near the N terminus of gH (57), whereas ADgO(GT1a) actually increased sensitivity of TR to AP86. Neutralization by either antibody on epithelial cells was not significantly affected, consistent with the notion that these antibodies can also neutralize by reacting to gH/gL/UL128-131. Again, the strain background exerted considerable influence over the effects of gO polymorphisms. For MT, it was ADgO(GT1a) that conferred resistance to 14-4b, and the other isoforms had little or no effect. The observed effects on neutralization on gH epitopes likely involve differences in how gO variable regions or associated glycans fold onto gH/gL to exert differential steric effects. Relatedly, the differential influence of gO isoforms in the two genetic backgrounds suggests epistasis involving the additive effects of gO polymorphisms with the more subtle gH polymorphisms, which together can differentially affect the global conformation of the gH/gL/gO trimer.

Previous analyses have suggested two groups of gH sequences defined by polymorphisms at the N terminus, including the AP86 epitope (57, 61). Of the strains represented in this study, TB, TR, and AD belong to the gH1 genotype and are sensitive to AP86, whereas ME, TN, and PH belong to gH2 genotype and are resistant to AP86. The differential effects of gO recombinants reported here raise questions about the

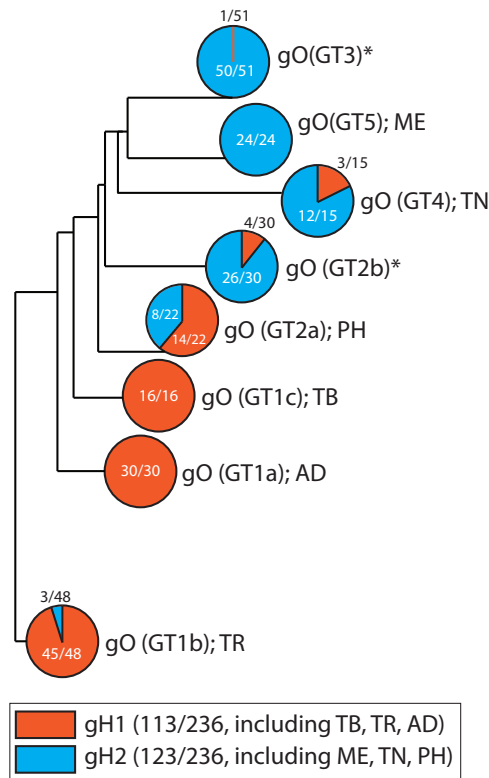


FIG 11 Association of gH and gO genotypes in 236 complete HCMV genome sequences in the NCBI database. Complete HCMV genome sequences were retrieved from the NCBI nucleotide database using the keywords filter <human herpesvirus type 5 complete genome>. The resulting set of 350 sequences was curated to remove duplicates or genomes missing any of the UL74(gO) and UL75(gH) open reading frames, generating a working set of 236 complete HCMV genomes, which were analyzed using MAFFT FFT-NS-i (v7.429) phylogeny software. UL74(gO) and UL75(gH) sequences were assigned to their respective genotype groups as defined previously: UL75(gH) genotypes 1 and 2 (57, 61) and UL74(gO) genotypes 1a, 1b, 1c, 2a, 2b, 3, 4, and 5 (10, 12). Shown is a phylogenetic tree of the 8 gO genotypes with the frequency of pairing with either gH1 or gH2. Asterisks indicate gO genotypes that were not analyzed in the experiments described herein.

combinations of gH and gO genotypes in HCMV circulating in human populations. The recently published genome sequence data sets from clinical specimens have been collected with short-read sequencing approaches, which allow sensitive detection of the various gH and gO genotypes within samples but not the combinations of the two ORFs on individual genomes (1, 3, 4, 6, 7). To address, this we analyzed 236 complete HCMV genome sequences of isolated strains and BAC clones in the NCBI database (Fig. 11). Approximately half the sequences were gH1 and the other half gH2. ADgO(GT1a) and TBgO(GT1c) genotypes were exclusively linked to gH1, whereas MEGO(GT5) was exclusively linked to gH2. Other gO genotypes were found mixed with both gH genotypes, but in most cases, disproportionately with one of the gH genotypes. These analyses agreed with those of Rasmussen et al., who suggested a strong linkage between gH1 and gO1 genotypes (note that their study predated the GT1a, -1b, and -1c subdivisions) (10). Thus, it appears that gH and gO genotypes are nonrandomly linked. This may be due in part to the adjacent position of UL74(gO) and UL75(gH) on the HCMV genome and the sequence diversity, together limiting the frequency of recombination, as suggested by the high linkage disequilibrium of this region reported by Lassalle et al. (3). In addition, our results may suggest linkage pressures based on functional compatibility of gH and gO. However, it is worth noting that among the more striking effects reported were the loss of cell-free infectivity and differential sensitivity to neutralization by gH antibodies of TR_ADgO(GT1a). Together with the fact that TR and AD are of the same gH genotype, these results suggest epistatic interplay of genetic variation of other loci with that of gH and gO.

In conclusion, we have shown that naturally occurring polymorphisms in the HCMV gO can have a dramatic influence on significant aspects of HCMV biology, including cell-free and cell-to-cell spread and neutralization by anti-gH antibodies. These effects could not be explained by changes to the levels of gH/gL complexes in the virion envelope but rather point to changes in the mechanism(s) of gH/gL/gO in the processes of cell-free and cell-to-cell spread. The associated epistasis with the global genetic background highlights a particular challenge for intervention approaches since humans can be superinfected with several combinations of HCMV genotypes and recombination may occur frequently (1–8). Moreover, these observations could help explain the incomplete protection observed for the natural antibody response against HCMV.

MATERIALS AND METHODS

Cell lines. Primary neonatal human dermal fibroblasts (nHDF; Thermo Fisher Scientific), MRC-5 fibroblasts (ATCC CCL-171; American Type Culture Collection, Manassas, VA), and HFFtet cells (which express the tetracycline [Tet] repressor protein; provided by Richard Stanton) (51) were grown in Dulbecco's modified Eagle's medium (DMEM; Thermo Fisher Scientific) supplemented with 6% heat-inactivated fetal bovine serum (FBS; Rocky Mountain Biologicals, Inc., Missoula, MT) and 6% bovine growth serum (BGS; Rocky Mountain Biologicals, Inc.) and with penicillin-streptomycin, gentamicin, and amphotericin B. Retinal pigment epithelial cells (ARPE19) (American Type Culture Collection) were grown in a 1:1 mixture of DMEM and Ham's F-12 medium (DMEM-F-12; Gibco) and supplemented with 10% FBS and with penicillin-streptomycin, gentamicin, and amphotericin B.

HCMV. All human cytomegaloviruses (HCMVs) were derived from bacterial artificial chromosome (BAC) clones. The BAC clone of TR was provided by Jay Nelson (Oregon Health and Sciences University, Portland, OR) (62). The BAC clone of Merlin (ME) (pAL1393), which carries tetracycline operator sequences in the transcriptional promoter of UL130 and UL131, was provided by Richard Stanton (51). All BAC clones were modified to express green fluorescent protein (GFP) by replacing the US11 ORF with the enhanced GFP (eGFP) gene under the control of the murine CMV major immediate early promoter. The constitutive expression of eGFP allows the monitoring of HCMV infection early and was strain independent. Infectious HCMV was recovered by electroporation of BAC DNA into MRC-5 fibroblasts, as described previously by Wille et al. (25), and then coculturing with nHDF or HFFtet cells. Cell-free HCMV stocks were produced by infecting HFF or HFFtet cells at 2 PFU per cell and harvesting culture supernatants at 8 to 10 days postinfection (when cells were still visually intact). Harvested culture supernatants were clarified by centrifugation at $1,000 \times g$ for 15 min. Stock aliquots were stored at -80°C . Freeze-thaw cycles were avoided. Infectious units (IU) were determined by infecting replicate cultures of nHDF or ARPE19 cells with serial 10-fold dilutions and using flow cytometry to count GFP-positive cells at 48 h postinfection.

Heterologous UL74(gO) recombinant HCMV. A modified, three step BAC en passant recombineering technique was performed (63, 64). In the first step, the endogenous UL74 ORF from the start codon to the stop codon of both TR and ME was replaced by a selectable marker. This necessary step was added to prevent formation of chimeric UL74 gene by internal recombination of the UL74 BAC sequence and the incoming heterologous UL74 ORF. A purified PCR product containing the ampicillin resistance selectable marker (AmpR) cassette from the pUC18 plasmid flanked by sequences homologous to 50 bp upstream and downstream of the TR or ME UL74 ORF was electroporated into the bacteria, recombination was induced, and the recombinant-positive bacteria were selected on medium containing ampicillin ($50 \mu\text{g/ml}$) and chloramphenicol ($12.5 \mu\text{g/ml}$). The primers used to produce the TR- and ME-specific AmpR PCR bands are as follows: For74TRamp, 5'-CATGGGAGCTTTTGTATCGTATTACGACAT TGCTGTTCCAGAACTTTTAcgcggaaccctattgttttattttctaaatac; For74MEamp, 5'-GATGGGAGCTTTTGTATC GTATTACGACATTGCTGCTCCAGAACTTTTAcgcggaaccctattgttttattttctaaatac; and Rev74amp (used for both TR and ME PCRs), 5'-CCAAACCACAAGGCAGACGGACGGTCTCTCTCTGTGATGGGttacc aatgcttaacagtgaggcacc. The lowercase nucleotides correspond to the AmpR gene from the pUC18 plasmid, and the uppercase nucleotides correspond to the TR and ME BAC sequences immediately upstream and downstream of the UL74 ORF.

In the second step, the AmpR cassette in the TR and ME first-step intermediate BACs was replaced with the UL74(gO) sequence from the heterologous strain containing the en passant cassette (63, 64). Briefly, *Escherichia coli* cultures were prepared for recombination as described above for step 1 and electroporated with purified PCR products containing the UL74 ORF from the TR or ME strain flanked by sequence homologous to 50 bp upstream and downstream of the opposite strain. The UL74 ORF also contained an inserted en passant cassette (an I-SceI site followed by a kanamycin resistance gene surrounded by a 50-bp duplication of the UL74 nucleotides of the insertion site). Transformed *E. coli* cells were induced for recombination and then selected for the swap of the UL74 en passant sequence into the BAC by growth on medium containing kanamycin ($50 \mu\text{g/ml}$) and chloramphenicol ($12.5 \mu\text{g/ml}$). A PCR analysis with primers located upstream and downstream of UL74 was used to confirm the swap of the AmpR cassette by the en passant cassette/UL74 gene.

In the third step, several sequencing validated colonies of the second step were subjected to the last step of the en passant recombineering, that is, an induction of both the I-SceI endonuclease and the recombinase (63, 64). The activity of these enzymes led to an intramolecular recombination in the UL74

sequence around the en passant cassette and thus the restoration of an uninterrupted, full-length UL74 ORF. The final heterologous UL74(gO) recombinants were verified by Sanger sequencing of PCR products using primers located upstream and downstream of the UL74 gene.

Antibodies. Monoclonal antibodies (MAbs) specific to HCMV major capsid protein (MCP), pp150, and gH (14-4b and AP86) were provided by Bill Britt (University of Alabama, Birmingham, AL) (35, 57, 65, 66). 14-4b and AP86 were purified by fast-performance liquid chromatography (FPLC) and quantified by the University of Montana Integrated Structural Biology Core Facility. Rabbit polyclonal serum against HCMV gL was described previously (9, 26).

Immunoblotting. HCMV cell-free virions were solubilized in 2% SDS–20 mM Tris-buffered saline (TBS) (pH 6.8). Insoluble material was cleared by centrifugation at $16,000 \times g$ for 15 min, and extracts were then boiled for 10 min. For reducing blots, dithiothreitol (DTT) was added to extracts to a final concentration of 25 mM. After separation by SDS-PAGE, proteins were transferred onto polyvinylidene difluoride (PVDF) membranes (Whatman) in a buffer containing 10 mM NaHCO_3 and 3 mM Na_2CO_3 (pH 9.9) plus 10% methanol. Transferred proteins were probed with MAbs or rabbit polyclonal antibodies, anti-rabbit or anti-mouse secondary antibodies conjugated with horseradish peroxidase (Sigma-Aldrich), and Pierce ECL-Western blotting substrate (Thermo Fisher Scientific). Chemiluminescence was detected using a Bio-Rad ChemiDoc MP imaging system. Band densities were quantified using Bio-Rad Image Lab v 5.1.

Quantitative PCR. Viral genomes were determined as described previously (26). Briefly, cell-free HCMV stocks were treated with DNase I before extraction of viral genomic DNA (PureLink viral RNA/DNA minikit; Life Technologies/Thermo Fisher Scientific). Primers specific for sequences within UL83 were used with the MyiQ real-time PCR detection system (Bio-Rad).

Flow cytometry. Recombinant GFP-expressing HCMV-infected cells were washed twice with phosphate-buffered saline (PBS) and lifted with trypsin. Trypsin was quenched with DMEM containing 10% FBS and cells were collected at $500 \times g$ for 5 min at room temperature (RT). Cells were fixed in PBS containing 2% paraformaldehyde for 10 min at RT and then washed and resuspended in PBS. Samples were analyzed using an AttuneNxT flow cytometer. Cells were identified using FSC-A and SSC-A, and single cells were gated using FSC-W and FSC-H. A BL-1 laser (488 nm) was used to identify GFP⁺ cells, and only cells with median GFP intensities 10-fold above background were considered positive.

Virus particle binding. nHDF or ARPE19 cells were seeded at density of 35,000 cells per cm² on chamber slides (Nunc Lab Tek II). Two days later, virus stocks were diluted with medium to equal numbers of virus particles based on genome quantification by qPCR. Binding of virus particles to the cells was allowed for 20 min at 37°C. Then the inoculum was removed, and the cells were washed once with medium to remove unbound virus before fixation and permeabilization with 80% acetone for 5 min. Bound virus particles were stained with an antibody against the capsid-associated tegument protein pp150 (65), which allowed detection of enveloped particles attached to the plasma membrane as well as internalized particles. For visualization, a goat anti-mouse Alexa Fluor 488 (Invitrogen) secondary antibody was used. Unbound secondary antibody was washed off before the chambers were removed and the cells were mounted with medium containing 4',6-diamidino-2-phenylindole (DAPI) (Fluoroshield) and sealed with a cover slide for later immunofluorescence analysis. Images were taken with a Leica DM5500 at 630-fold magnification. For each sample, 10 images with 4 to 6 cells per image were taken and the number of cell nuclei as well as the number of virus particles was determined using ImageJ Fiji software (v 1.0). Three independent virus stocks were tested in 3 independent experiments.

Antibody neutralization assays. Equal numbers of nHDF-derived cell-free parental viruses and heterologous gO recombinants were incubated with multiple concentrations of anti-gH MAb 14-4b or AP86 for 1 h at RT and then plated on nHDF or ARPE19 cells for 4 h at 37°C. Cells were then cultured in the appropriate growth medium supplemented with 2% FBS. After 2 days, cells were detected from the dish and fixed for flow cytometry analyses. Each antibody concentration was tested in triplicate, and 3 independent experiments were conducted.

ACKNOWLEDGMENTS

We are grateful to Bill Britt, David Johnson, Jay Nelson, and Richard Stanton for generously supplying HCMV BAC clones, antibodies, and cell lines as indicated in Materials and Methods and to members of the Ryckman laboratory for support and insightful discussions. We also thank Ekaterina Voronina and Mary Ellenbecker of the University of Montana for assistance with immunofluorescent microscopy, the staff of the University of Montana Center for Biomolecular Structure and Dynamics Integrated Structural Biology Core Facility for help purifying monoclonal antibodies, and the staff of the University of Montana Flow Cytometry Core of the Center for Environmental Health Sciences for assistance with flow cytometry.

This work was supported by grant from the National Institutes of Health to B.J.R. (R01AI097274), a fellowship from the German Research Foundation (DFG) to C.S. (STE 2835/1-1), a fellowship from the American Heart Association to E.P.S. (17POST33350043), and a National Institutes of Health CoBRE award to the Center for Biomolecular Structure and Dynamics at University of Montana (PG20GM103546).

Experiments were designed by B.J.R., L.Z.D., C.S., and E.P.S. and performed by L.Z.

and C.S. Critical reagents were developed by L.Z.D., J.-M.L., and Q.Y. Data were analyzed and the manuscript was prepared by B.J.R., L.Z.D., C.S., Q.Y., E.P.S., and J.-M.L.

REFERENCES

- Cudini J, Roy S, Houldcroft CJ, Bryant JM, Depledge DP, Tutill H, Veys P, Williams R, Worth AJ, Tamuri AU, Goldstein RA, Breuer J. 2019. Human cytomegalovirus haplotype reconstruction reveals high diversity due to superinfection and evidence of within-host recombination. *Proc Natl Acad Sci U S A* 116:5693–5698. <https://doi.org/10.1073/pnas.1818130116>.
- Hage E, Wilkie GS, Linnenweber-Held S, Dhingra A, Suárez NM, Schmidt JJ, Kay-Fedorov PC, Mischak-Weissinger E, Heim A, Schwarz A, Schulz TF, Davison AJ, Ganzenmueller T. 2017. Characterization of human cytomegalovirus genome diversity in immunocompromised hosts by whole-genome sequencing directly from clinical specimens. *J Infect Dis* 215:1673–1683. <https://doi.org/10.1093/infdis/jix157>.
- Lassalle F, Depledge DP, Reeves MB, Brown AC, Christiansen MT, Tutill HJ, Williams RJ, Einer-Jensen K, Holdstock J, Atkinson C, Brown JR, van Loenen FB, Clark DA, Griffiths PD, Verjans GMGM, Schutten M, Milne RSB, Balloux F, Breuer J. 2016. Islands of linkage in an ocean of pervasive recombination reveals two-speed evolution of human cytomegalovirus genomes. *Virus Evol* 2:vev017. <https://doi.org/10.1093/ve/vev017>.
- Renzette N, Bhattacharjee B, Jensen JD, Gibson L, Kowalik TF. 2011. Extensive genome-wide variability of human cytomegalovirus in congenitally infected infants. *PLoS Pathog* 7:e1001344. <https://doi.org/10.1371/journal.ppat.1001344>.
- Renzette N, Gibson L, Bhattacharjee B, Fisher D, Schleiss MR, Jensen JD, Kowalik TF. 2013. Rapid intrahost evolution of human cytomegalovirus is shaped by demography and positive selection. *PLoS Genet* 9:e1003735. <https://doi.org/10.1371/journal.pgen.1003735>.
- Sijmons S, Thys K, Mbong Ngwese M, Van Damme E, Dvorak J, Van Look M, Li G, Tachezy R, Busson L, Aerssens J, Van Ranst M, Maes P. 2015. High-throughput analysis of human cytomegalovirus genome diversity highlights the widespread occurrence of gene-disrupting mutations and pervasive recombination. *J Virol* 89:7673–7695. <https://doi.org/10.1128/JVI.00578-15>.
- Suárez NM, Musonda KG, Escriva E, Njenga M, Agbueze A, Camiolo S, Davison AJ, Gompels UA. 2019. Multiple-strain infections of human cytomegalovirus with high genomic diversity are common in breast milk from human immunodeficiency virus-infected women in Zambia. *J Infect Dis* 220:792–801. <https://doi.org/10.1093/infdis/jiz209>.
- Suárez NM, Wilkie GS, Hage E, Camiolo S, Holton M, Hughes J, Maabar M, Vattipally SB, Dhingra A, Gompels UA, Wilkinson GWG, Baldanti F, Furione M, Lillier D, Arossa A, Ganzenmueller T, Gerna G, Hubáček P, Schulz TF, Wolf D, Zavattoni M, Davison AJ. 2019. Human cytomegalovirus genomes sequenced directly from clinical material: variation, multiple-strain infection, recombination, and gene loss. *J Infect Dis* 220:781–791. <https://doi.org/10.1093/infdis/jiz208>.
- Zhou M, Yu Q, Wechsler A, Ryckman BJ. 2013. Comparative analysis of gO isoforms reveals that strains of human cytomegalovirus differ in the ratio of gH/gL/gO and gH/gL/UL128-131 in the virion envelope. *J Virol* 87:9680–9690. <https://doi.org/10.1128/JVI.01167-13>.
- Rasmussen L, Geissler A, Cowan C, Chase A, Winters M. 2002. The genes encoding the gCIII complex of human cytomegalovirus exist in highly diverse combinations in clinical isolates. *J Virol* 76:10841–10848. <https://doi.org/10.1128/jvi.76.21.10841-10848.2002>.
- Stanton R, Westmoreland D, Fox JD, Davison AJ, Wilkinson GW. 2005. Stability of human cytomegalovirus genotypes in persistently infected renal transplant recipients. *J Med Virol* 75:42–46. <https://doi.org/10.1002/jmv.20235>.
- Mattick C, Dewin D, Polley S, Sevilla-Reyes E, Pignatelli S, Rawlinson W, Wilkinson G, Dal Monte P, Gompels UA. 2004. Linkage of human cytomegalovirus glycoprotein gO variant groups identified from worldwide clinical isolates with gN genotypes, implications for disease associations and evidence for N-terminal sites of positive selection. *Virology* 318:582–597. <https://doi.org/10.1016/j.virol.2003.09.036>.
- Görzer I, Guelly C, Trajanoski S, Puchhammer-Stöckl E. 2010. Deep sequencing reveals highly complex dynamics of human cytomegalovirus genotypes in transplant patients over time. *J Virol* 84:7195–7203. <https://doi.org/10.1128/JVI.00475-10>.
- Cooper RS, Heldwein EE. 2015. Herpesvirus gB: a finely tuned fusion machine. *Viruses* 7:6552–6569. <https://doi.org/10.3390/v7122957>.
- Heldwein EE. 2016. gH/gL supercomplexes at early stages of herpesvirus entry. *Curr Opin Virol* 18:1–8. <https://doi.org/10.1016/j.coviro.2016.01.010>.
- Connolly SA, Jackson JO, Jardetzky TS, Longnecker R. 2011. Fusing structure and function: a structural view of the herpesvirus entry machinery. *Nat Rev Microbiol* 9:369–381. <https://doi.org/10.1038/nrmicro2548>.
- Wang D, Shenk T. 2005. Human cytomegalovirus virion protein complex required for epithelial and endothelial cell tropism. *Proc Natl Acad Sci U S A* 102:18153–18158. <https://doi.org/10.1073/pnas.0509201102>.
- Li L, Nelson JA, Britt WJ. 1997. Glycoprotein H-related complexes of human cytomegalovirus: identification of a third protein in the gCIII complex. *J Virol* 71:3090–3097. <https://doi.org/10.1128/JVI.71.4.3090-3097.1997>.
- Huber MT, Compton T. 1997. Characterization of a novel third member of the human cytomegalovirus glycoprotein H-glycoprotein L complex. *J Virol* 71:5391–5398. <https://doi.org/10.1128/JVI.71.7.5391-5398.1997>.
- Vanarsdall AL, Howard PW, Wisner TW, Johnson DC. 2016. Human cytomegalovirus gH/gL forms a stable complex with the fusion protein gB in virions. *PLoS Pathog* 12:e1005564. <https://doi.org/10.1371/journal.ppat.1005564>.
- Hahn G, Revello MG, Patrone M, Percivalle E, Campanini G, Sarasini A, Wagner M, Gallina A, Milanese G, Koszinowski U, Baldanti F, Gerna G. 2004. Human cytomegalovirus UL131-128 genes are indispensable for virus growth in endothelial cells and virus transfer to leukocytes. *J Virol* 78:10023–10033. <https://doi.org/10.1128/JVI.78.18.10023-10033.2004>.
- Jiang XJ, Adler B, Sampaio KL, Digel M, Jahn G, Ettischer N, Stierhof YD, Scrivano L, Koszinowski U, Mach M, Sinzger C. 2008. UL74 of human cytomegalovirus contributes to virus release by promoting secondary envelopment of virions. *J Virol* 82:2802–2812. <https://doi.org/10.1128/JVI.01550-07>.
- Ryckman BJ, Jarvis MA, Drummond DD, Nelson JA, Johnson DC. 2006. Human cytomegalovirus entry into epithelial and endothelial cells depends on genes UL128 to UL150 and occurs by endocytosis and low-pH fusion. *J Virol* 80:710–722. <https://doi.org/10.1128/JVI.80.2.710-722.2006>.
- Wang D, Shenk T. 2005. Human cytomegalovirus UL131 open reading frame is required for epithelial cell tropism. *J Virol* 79:10330–10338. <https://doi.org/10.1128/JVI.79.16.10330-10338.2005>.
- Wille PT, Knoche AJ, Nelson JA, Jarvis MA, Johnson DC. 2010. A human cytomegalovirus gO-null mutant fails to incorporate gH/gL into the virion envelope and is unable to enter fibroblasts and epithelial and endothelial cells. *J Virol* 84:2585–2596. <https://doi.org/10.1128/JVI.02249-09>.
- Zhou M, Lanchy JM, Ryckman BJ. 2015. Human cytomegalovirus gH/gL/gO promotes the fusion step of entry into all cell types, whereas gH/gL/UL128-131 broadens virus tropism through a distinct mechanism. *J Virol* 89:8999–9009. <https://doi.org/10.1128/JVI.01325-15>.
- Laib Sampaio K, Stegmann C, Brizic I, Adler B, Stanton RJ, Sinzger C. 2016. The contribution of pUL74 to growth of human cytomegalovirus is masked in the presence of RL13 and UL128 expression. *J Gen Virol* 97:1917–1927. <https://doi.org/10.1099/jgv.0.000475>.
- Wu K, Oberstein A, Wang W, Shenk T. 2018. Role of PDGF receptor- α during human cytomegalovirus entry into fibroblasts. *Proc Natl Acad Sci U S A* 115:E9889–E9898. <https://doi.org/10.1073/pnas.1806305115>.
- E X, Meraner P, Lu P, Perreira JM, Aker AM, McDougall WM, Zhuge R, Chan GC, Gerstein RM, Caposio P, Yurochko AD, Brass AL, Kowalik TF. 2019. OR1411 is a receptor for the human cytomegalovirus pentameric complex and defines viral epithelial cell tropism. *Proc Natl Acad Sci U S A* 116:7043–7052. <https://doi.org/10.1073/pnas.1814850116>.
- Kabanova A, Marcandalli J, Zhou T, Bianchi S, Baxa U, Tsybovsky Y, Lillier D, Silacci-Fregni C, Foglierini M, Fernandez-Rodriguez BM, Druz A, Zhang B, Geiger R, Pagani M, Sallusto F, Kwong PD, Corti D, Lanzavecchia A, Perez L. 2016. Platelet-derived growth factor- α receptor is the cellular receptor for human cytomegalovirus gHgLgO trimer. *Nat Microbiol* 1:16082. <https://doi.org/10.1038/nmicrobiol.2016.82>.
- Martinez-Martin N, Marcandalli J, Huang CS, Arthur CP, Perotti M, Foglierini M, Ho H, Dosey AM, Shriver S, Payandeh J, Leitner A, Lanzavecchia A, Perez L, Ciferrì C. 2018. An unbiased screen for human cytomegalovirus identifies neuropilin-2 as a central viral receptor. *Cell* 174:1158–1171.e19. <https://doi.org/10.1016/j.cell.2018.06.028>.

32. Wu Y, Prager A, Boos S, Resch M, Brizic I, Mach M, Wildner S, Scrivano L, Adler B. 2017. Human cytomegalovirus glycoprotein complex gH/gL/gO uses PDGFR- α as a key for entry. *PLoS Pathog* 13:e1006281. <https://doi.org/10.1371/journal.ppat.1006281>.
33. Stegmann C, Hochdorfer D, Lieber D, Subramanian N, Stöhr D, Laib Sampaio K, Sinzger C. 2017. A derivative of platelet-derived growth factor receptor alpha binds to the trimer of human cytomegalovirus and inhibits entry into fibroblasts and endothelial cells. *PLoS Pathog* 13:e1006273. <https://doi.org/10.1371/journal.ppat.1006273>.
34. Vanarsdall AL, Ryckman BJ, Chase MC, Johnson DC. 2008. Human cytomegalovirus glycoproteins gB and gH/gL mediate epithelial cell-cell fusion when expressed either in cis or in trans. *J Virol* 82:11837–11850. <https://doi.org/10.1128/JVI.01623-08>.
35. Bogner E, Reschke M, Reis B, Reis E, Britt W, Radsak K. 1992. Recognition of compartmentalized intracellular analogs of glycoprotein H of human cytomegalovirus. *Arch Virol* 126:67–80. <https://doi.org/10.1007/bf01309685>.
36. Chiuppesi F, Wussow F, Johnson E, Bian C, Zhuo M, Rajakumar A, Barry PA, Britt WJ, Chakraborty R, Diamond DJ. 2015. Vaccine-derived neutralizing antibodies to the human cytomegalovirus gH/gL pentamer potently block primary cytotrophoblast infection. *J Virol* 89:11884–11898. <https://doi.org/10.1128/JVI.01701-15>.
37. Fouts AE, Chan P, Stephan JP, Vandlen R, Feierbach B. 2012. Antibodies against the gH/gL/UL128/UL130/UL131 complex comprise the majority of the anti-cytomegalovirus (anti-CMV) neutralizing antibody response in CMV hyperimmune globulin. *J Virol* 86:7444–7447. <https://doi.org/10.1128/JVI.00467-12>.
38. Fouts AE, Comps-Agrar L, Stengel KF, Ellerman D, Schoeffler AJ, Warming S, Eaton DL, Feierbach B. 2014. Mechanism for neutralizing activity by the anti-CMV gH/gL monoclonal antibody MSL-109. *Proc Natl Acad Sci U S A* 111:8209–8214. <https://doi.org/10.1073/pnas.1404653111>.
39. Gerna G, Percivalle E, Perez L, Lanzavecchia A, Lillieri D. 2016. Monoclonal antibodies to different components of the human cytomegalovirus (HCMV) pentamer gH/gL/pUL128L and trimer gH/gL/gO as well as antibodies elicited during primary HCMV infection prevent epithelial cell syncytium formation. *J Virol* 90:6216–6223. <https://doi.org/10.1128/JVI.00121-16>.
40. Kabanova A, Perez L, Lillieri D, Marcandalli J, Agatic G, Becattini S, Preite S, Fuschillo D, Percivalle E, Sallusto F, Gerna G, Corti D, Lanzavecchia A. 2014. Antibody-driven design of a human cytomegalovirus gHgLpUL128L subunit vaccine that selectively elicits potent neutralizing antibodies. *Proc Natl Acad Sci U S A* 111:17965–17970. <https://doi.org/10.1073/pnas.1415310111>.
41. Nokta M, Tolpin MD, Nadler PI, Pollard RB. 1994. Human monoclonal anti-cytomegalovirus (CMV) antibody (MSL 109): enhancement of in vitro foscarnet- and ganciclovir-induced inhibition of CMV replication. *Antiviral Res* 24:17–26. [https://doi.org/10.1016/0166-3542\(94\)90048-5](https://doi.org/10.1016/0166-3542(94)90048-5).
42. Vanarsdall AL, Chin AL, Liu J, Jardetzky TS, Mudd JO, Orloff SL, Streblow D, Mussi-Pinhata MM, Yamamoto AY, Duarte G, Britt WJ, Johnson DC. 2019. HCMV trimer- and pentamer-specific antibodies synergize for virus neutralization but do not correlate with congenital transmission. *Proc Natl Acad Sci U S A* 116:3728–3733. <https://doi.org/10.1073/pnas.1814835116>.
43. Wussow F, Chiuppesi F, Martinez J, Campo J, Johnson E, Flechsig C, Newell M, Tran E, Ortiz J, La Rosa C, Herrmann A, Longmate J, Chakraborty R, Barry PA, Diamond DJ. 2014. Human cytomegalovirus vaccine based on the envelope gH/gL pentamer complex. *PLoS Pathog* 10:e1004524. <https://doi.org/10.1371/journal.ppat.1004524>.
44. Wei X, Decker JM, Wang S, Hui H, Kappes JC, Wu X, Salazar-Gonzalez JF, Salazar MG, Kilby JM, Saag MS, Komarova NL, Nowak MA, Hahn BH, Kwong PD, Shaw GM. 2003. Antibody neutralization and escape by HIV-1. *Nature* 422:307–312. <https://doi.org/10.1038/nature01470>.
45. Kropff B, Burkhardt C, Schott J, Nentwich J, Fisch T, Britt W, Mach M. 2012. Glycoprotein N of human cytomegalovirus protects the virus from neutralizing antibodies. *PLoS Pathog* 8:e1002999. <https://doi.org/10.1371/journal.ppat.1002999>.
46. Jiang XJ, Sampaio KL, Ettischer N, Stierhof YD, Jahn G, Kropff B, Mach M, Sinzger C. 2011. UL74 of human cytomegalovirus reduces the inhibitory effect of gH-specific and gB-specific antibodies. *Arch Virol* 156:2145–2155. <https://doi.org/10.1007/s00705-011-1105-x>.
47. Cui X, Freed DC, Wang D, Qiu P, Li F, Fu TM, Kauvar LM, McVoy MA. 2017. Impact of antibodies and strain polymorphisms on cytomegalovirus entry and spread in fibroblasts and epithelial cells. *J Virol* 91:e01650-16. <https://doi.org/10.1128/JVI.01650-16>.
48. Zhang L, Zhou M, Stanton R, Kamil J, Ryckman BJ. 2018. Expression levels of glycoprotein O (gO) vary between strains of human cytomegalovirus, influencing the assembly of gH/gL complexes and virion infectivity. *J Virol* 92:e00606-18. <https://doi.org/10.1128/JVI.00606-18>.
49. Kalsler J, Adler B, Mach M, Kropff B, Puchhammer-Stöckl E, Görzer I. 2017. Differences in growth properties among two human cytomegalovirus glycoprotein O genotypes. *Front Microbiol* 8:1609. <https://doi.org/10.3389/fmicb.2017.01609>.
50. Murrell I, Bedford C, Ladell K, Miners KL, Price DA, Tomasec P, Wilkinson GW, Stanton RJ. 2017. The pentameric complex drives immunologically covert cell-cell transmission of wild-type human cytomegalovirus. *Proc Natl Acad Sci U S A* 114:6104–6109. <https://doi.org/10.1073/pnas.1704809114>.
51. Stanton RJ, Baluchova K, Dargan DJ, Cunningham C, Sheehy O, Seirafian S, McSharry BP, Neale ML, Davies JA, Tomasec P, Davison AJ, Wilkinson GW. 2010. Reconstruction of the complete human cytomegalovirus genome in a BAC reveals RL13 to be a potent inhibitor of replication. *J Clin Invest* 120:3191–3208. <https://doi.org/10.1172/JCI42955>.
52. Murrell I, Wilkie GS, Davison AJ, Statkute E, Fielding CA, Tomasec P, Wilkinson GW, Stanton RJ. 2016. Genetic stability of bacterial artificial chromosome-derived human cytomegalovirus during culture in vitro. *J Virol* 90:3929–3943. <https://doi.org/10.1128/JVI.02858-15>.
53. Vanarsdall AL, Wisner TW, Lei H, Kazlauskas A, Johnson DC. 2012. PDGF receptor- α does not promote HCMV entry into epithelial and endothelial cells but increased quantities stimulate entry by an abnormal pathway. *PLoS Pathog* 8:e1002905. <https://doi.org/10.1371/journal.ppat.1002905>.
54. Liu J, Jardetzky TS, Chin AL, Johnson DC, Vanarsdall AL. 2018. The human cytomegalovirus trimer and pentamer promote sequential steps in entry into epithelial and endothelial cells at cell surfaces and endosomes. *J Virol* 92:e01336-18. <https://doi.org/10.1128/JVI.01336-18>.
55. Murrell I, Tomasec P, Wilkie GS, Dargan DJ, Davison AJ, Stanton RJ. 2013. Impact of sequence variation in the UL128 locus on production of human cytomegalovirus in fibroblast and epithelial cells. *J Virol* 87:10489–10500. <https://doi.org/10.1128/JVI.01546-13>.
56. Schultz EP, Lanchy JM, Ellerbeck EE, Ryckman BJ. 2015. Scanning mutagenesis of human cytomegalovirus glycoprotein gH/gL. *J Virol* 90:2294–2305. <https://doi.org/10.1128/JVI.01875-15>.
57. Urban M, Britt W, Mach M. 1992. The dominant linear neutralizing antibody-binding site of glycoprotein gp86 of human cytomegalovirus is strain specific. *J Virol* 66:1303–1311. <https://doi.org/10.1128/JVI.66.3.1303-1311.1992>.
58. Ourahmane A, Cui X, He L, Catron M, Dittmer DP, Al Qaffasaa A, Schleiss MR, Hertel L, McVoy MA. 2019. Inclusion of antibodies to cell culture media preserves the integrity of genes encoding RL13 and the pentameric complex components during fibroblast passage of human cytomegalovirus. *Viruses* 11:221. <https://doi.org/10.3390/v11030221>.
59. Scrivano L, Sinzger C, Nitschko H, Koszinowski UH, Adler B. 2011. HCMV spread and cell tropism are determined by distinct virus populations. *PLoS Pathog* 7:e1001256. <https://doi.org/10.1371/journal.ppat.1001256>.
60. Stegmann C, Rothmund F, Laib Sampaio K, Adler B, Sinzger C. 2019. The N terminus of human cytomegalovirus glycoprotein O is important for binding to the cellular receptor PDGFR α . *J Virol* 93:e00138-19. <https://doi.org/10.1128/JVI.00138-19>.
61. Chou S. 1992. Molecular epidemiology of envelope glycoprotein H of human cytomegalovirus. *J Infect Dis* 166:604–607. <https://doi.org/10.1093/infdis/166.3.604>.
62. Murphy E, Yu D, Grimwood J, Schmutz J, Dickson M, Jarvis MA, Hahn G, Nelson JA, Myers RM, Shenk TE. 2003. Coding potential of laboratory and clinical strains of human cytomegalovirus. *Proc Natl Acad Sci U S A* 100:14976–14981. <https://doi.org/10.1073/pnas.2136652100>.
63. Tischer BK, von Einem J, Kaufner B, Osterrieder N. 2006. Two-step red-mediated recombination for versatile high-efficiency markerless DNA manipulation in *Escherichia coli*. *Biotechniques* 40:191–197. <https://doi.org/10.2144/000112096>.
64. Tischer BK, Smith GA, Osterrieder N. 2010. En passant mutagenesis: a two step markerless red recombination system. *Methods Mol Biol* 634:421–430. https://doi.org/10.1007/978-1-60761-652-8_30.
65. Sanchez V, Greis KD, Sztul E, Britt WJ. 2000. Accumulation of virion tegument and envelope proteins in a stable cytoplasmic compartment during human cytomegalovirus replication: characterization of a potential site of virus assembly. *J Virol* 74:975–986. <https://doi.org/10.1128/jvi.74.2.975-986.2000>.
66. Chee M, Rudolph SA, Plachter B, Barrell B, Jahn G. 1989. Identification of the major capsid protein gene of human cytomegalovirus. *J Virol* 63:1345–1353. <https://doi.org/10.1128/JVI.63.3.1345-1353.1989>.